4th International Workshop on Physics with Trapped Charged Particles (IWPTCP-26), IUAC, New Delhi

Wednesday, 25 November 2026 - Friday, 27 November 2026

Maharishi Kanad Auditorium, IUAC

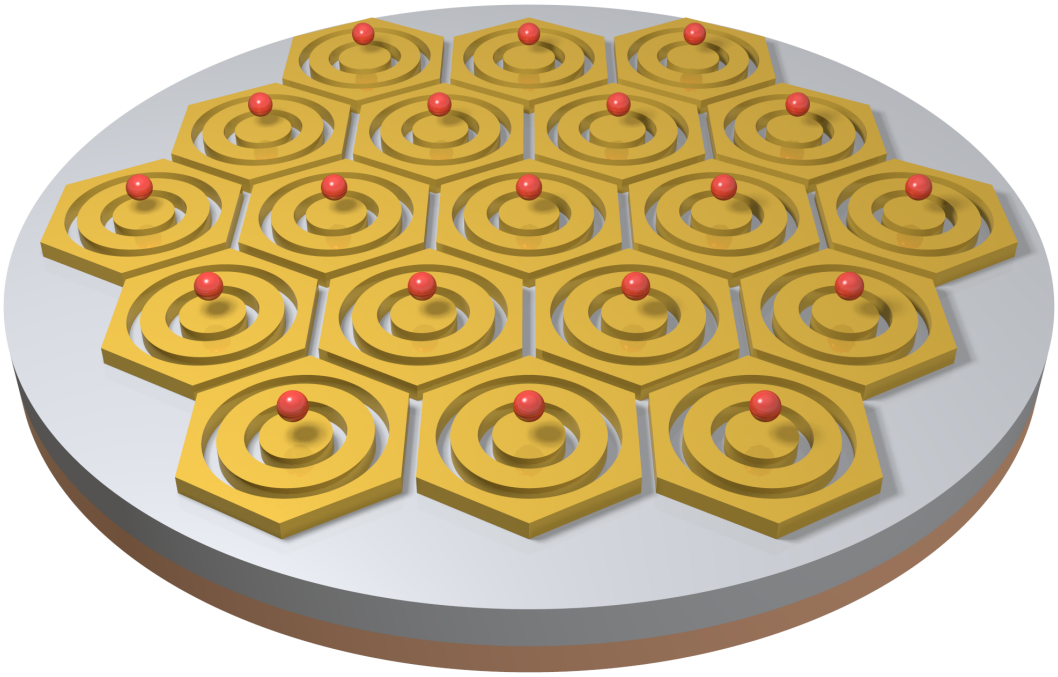

Book of Abstracts

It is our great pleasure to welcome you to the **4th International Workshop on Physics with Trapped Charged Particles (IWPTCP-2026)**, held at the Inter-University Accelerator Centre (IUAC), New Delhi, from 25 to 27 November 2026.

IWPTCP-2026 focuses on the use of ion and electron traps for advancing fundamental physics, precision spectroscopy, quantum computing and quantum information science. Trapped ions and electrons have emerged as some of the most promising platforms for scalable quantum computing, quantum simulation, high-fidelity quantum control and precision measurements. The workshop also highlights research on highly charged ions, quantum electrodynamics (QED), antimatter, frequency standards and atomic collisions.

Building on the previous editions of this series, including IWPTCP-2024 at IUAC, the workshop brings together leading experimentalists and theoreticians from India and abroad to discuss the latest advances, exchange ideas, and foster collaborations that will shape future developments in quantum technologies and fundamental physics. The scientific programme comprises invited talks by experts from leading institutions in India and abroad, together with contributed presentations, many of them by students and early-career researchers.

Topics of the workshop

- Highly charged ions in ion traps
- Ion/electron trap based quantum computing
- Radioactive isotopes in traps
- Ion–atom–molecular collisions
- Electron collisions
- Radiative lifetimes of atomic metastable states
- Precision spectroscopy and frequency standards

This Book of Abstracts contains the abstracts of the invited talks and contributed presentations. We thank all speakers and participants for their contributions, and the members of the organizing committee and the staff of IUAC for their efforts in making this workshop possible. We gratefully acknowledge the support of the Inter-University Accelerator Centre, the Anusandhan National Research Foundation (ANRF) and the Council of Scientific and Industrial Research (CSIR).

We wish you a stimulating and enjoyable workshop and a pleasant stay in New Delhi.

Dr. Sugam Kumar
Convener, IWPTCP-2026
on behalf of the Organizing Committee
Inter-University Accelerator Centre, New Delhi

Program Schedule

25 November 2026

08:00-09:30	**Registration**	
09:30-10:30	**Inaugral Ceremony**	
10:30-11:00	Planar trap arrays for quantum information processing and simulation with two dimensional charged particle crystals	Dr. Manuel Vogel, GSI, Darmstadt, Germany
11:00-11:50	**High Tea**	
Session 1	**Chair: Prof. Wolfgang Quint**	
11:50-12:30	A Scalable 2D Planar Penning Trap Architecture for Trapped-Electron Quantum Computing	IUAC, New Delhi, India
12:30-13:00	Geonium Chip: Quantum Microwave Technology with Trapped Electrons	Prof. Jose Luis Verdú Galiana, University of Sussex, UK
13:00-14:20	**Lunch**	
Session 2	**Chair: Prof. Sadiq Rangwala**	
14:20-15:00	Quantum computing with trapped ions (Online Talk)	Prof. Ferdinand Schmidt-Kaler, JGU Mainz, Germany
15:00-15:30	Rack-assembled, high-uptime $^{171}Yb^{+}$ single-ion optical clock with systematic uncertainty below 2×10^{-17} and instability below 4×10^{-18}	Dr. Juergen Stuhler, TOPTICA Photonics, Germany
15:30-16:00	**Tea/Coffee**	
Session 3	**Chair: Prof. Lokesh C Tribedi**	
16:00-16:30	Large scale quantum simulation with trapped ions	Prof. Manoj Kumar Joshi, SUTD, Singapore
16:30-16:50	Quantum computing with X- junction for 2D navigation of trapped ion qubits	Dr. Salvi Mohandas, Johannes Gutenberg-Universität Mainz
16:50-17:10	High-Harmonicity Planar Penning Traps for Single-Electron Qubits	Mr. Kedar Mal IUAC, New Delhi
17:10-17:30	Induced charge Coupling frequency of axial motion of two electrons trapped separately in a 2D Planar Penning Trap	Dr. Geetu Narang, Punjab University, Chandigarh
19:00-20:00	**Evening Talk** Building Hardware Ecosystem for Qantum Computing Dr. L Venkata Subramaniam, Founder Director, Qubit Force	
20:00-	**Directors dinner**	

Program Schedule

26 November 2026

Session 4	**Chair: Prof. Jose Luis Verdú Galiana**	
09:00-09:30	Seeking advantage in Quantum-Classical Machine Learning with trapped ion system	Prof. Manas Mukherjee NUS / CQT, Singapore
09:30-10:00	Developing a high-fidelity calcium-ion quantum computer	Dr. Sapam Ranjita Chanu IIT Kanpur, India
10:00-10:30	Quantifying the rate for rare events using trapped ions	Prof. Sadiq Rangwala RRI, Bangalore, India
10:30-11:00	**Tea/Coffee**	
Session 5	**Chair: Dr. Manuel Vogel**	
11:00-11:30	HiThorSpectrap- A Penning Trap to faciliate a Thorium Nuclear Clock	Dr. Stefan Ringleb, Friedrich Schiller University, Jena, Germany
11:30-12:00	Trapped ion based Optical Atomic Clock; A possible way of re-defining SI second	Dr. Subhasis Panja CSIR-NPL, New Delhi, India
12:00-12:30	Direct Measurement of Zero-point energy of Quantum harmonic Oscillator in Penning Trap	Prof. Wolfgang Quint GSI, Darmstadt, Germany
12:30-13:30	**Lunch**	
13:30-15:00	**POSTER SESSION**	
Session 6	**Chair: Prof. Saptarishi Chaudhury**	
15:00-15:30	Stringent Tests of the Standard Model via High-Precision Measurements at ALPHATRAP and LIONTRAP	Dr. Fabian Heiße, Max Planck Institute for Nuclear Physics, Germany (Online Talk)
15:30-16:00	Near threshold statistical dissociation of quinoline cations using action spectroscopy in cryogenic storage	Prof. Umesh R. Kadhane IIST, Thiruvananthapuram, India
16:00-16:30	**Tea/Coffee**	
Session 7	**Industry session, Chair: Dr. C. P. Safvan**	
16:30-16:50	Solutions for Quantum technologies	Mr. Tapan Sharda, New Age Instruments
16:50-17:10	Multimodal Quantum Computing approaches - Hardware Software co-design	Dr. Naga Chaitanya Kosanam, TriQuanta Lab, Hyderabad
17:10-17:30	Development of indigenous Precision power supply for quantum computing	Dr. Sugam Kumar QUTE Electronics, New Delhi
20:00-	**Conference Dinner**	

Program Schedule

27 November 2026

Session 8	**Chair: Dr. Parnika Das**	
09:00-09:30	Quantum Sensing with Neutral atoms and high Precision Diode Lasers	Prof. Bodhaditya Santra, IIT Delhi, India
09:30-10:00	Engineering Quantum Systems with Laser-Cooled Neutral Atoms	Prof. Saptarishi Chaudhury RRI, Bengaluru
10:00-10:20	Photostability of isolated nucleotides under ultraviolet radiation	Mr. Abheek Roy IISER Tirupati
10:20-10:40	Dynamical States of Driven Few-Ion Crystals	Vaibhav Mahendrakar RRI Bengaluru
10:40-11:00	Kinetic Monte Carlo Modelling of Recurrent Fluorescence in PAH Cations for the Delhi Penning Trap	Shravan Rajesh Kale, IIST, Thiruvananthapuram
11:00-11:30	**Tea/Coffee**	
Session 9	**Chair: Dr. Bodhaditya Santra**	
11:30-12:00	Observation of spontaneous N-bearing PAH formation using an ion trap: A new formation pathway in the interstellar medium	Prof. G. Aravind IIT Madras, India (Online Talk)
12:00-12:30	Effect of imperfections on the thermometry of ions stored in a 16-pole radiofrequency ion trap	Dr. S. Sunil Kumar IISER, Tirupati, India
12:30-14:00	**Lunch**	
Session 10	**Chair: Prof. Manas Mukherjee**	
14:00-14:30	Penning-Trap Techniques for Nuclear Decay and Precision Nuclear Spectroscopy	Dr. Parnika Das VECC, Kolkata, India
14:30-15:00	Non-Invasive Room-Temperature Detection of a Single Trapped Electron in VECC Penning Trap	Dr. Arindam Sikdar VECC, Kolkata
15:00-15:20	Identification and consolidation of decay hierarchy of statistical fragmentation network in aromatic molecules and their fragments	Ms. Binduja Panja, IIST, Thiruvananthapuram
15:20-15:50	**Closing**	
15:50 -	**Tea / Coffee**	

Contents

I Invited Talks **1**

Planar Trap Arrays for Quantum Information Processing and Simulation with two-dimensional Charged-Particle Crystals . . . 3

A Scalable 2D Planar Penning Trap Architecture for Trapped-Electron Quantum Computing . . . 4

Trapped ion quantum computing . . . 5

Rack-assembled, high-uptime $^{171}Yb^{+}$ single-ion optical clock with systematic uncertainty below $2x10^{-17}$ and instability below $4x10^{-18}$ . . . 6

Quantum physics with trapped ions . . . 7

Seeking advantage in Quantum-Classical Machine Learning with trapped ion system . . . 8

Developing a high-fidelity calcium-ion quantum computer . . . 9

Quantifying the rate for rare events using trapped ions . . . 10

HiThor@Spectrap - A Penning Trap to faciliate a Thorium Nuclear Clock . . . 11

Trapped Ion based Optical Atomic Clock: A Possible Way of Redefining SI Second . . . 12

Zero-Point Energy of the Electron in a Penning Trap by Photo-Detachment Laser Spectroscopy . . . 13

Near threshold statistical dissociation of quinoline cations using action spectroscopy in cryogenic storage 14

Quantum Sensing with Neutral Atoms and High-Precision Diode Lasers . . . 15

Detecting Trapped Atoms with Minimal Disturbance: Real-Time Readout through Spin Noise . . . 16

Observation of spontaneous N-bearing PAH formation using an ion trap: A new formation pathway in the interstellar medium . . . 17

Effect of imperfections on the thermometry of ions stored in a 16-pole radiofrequency ion trap . . . 18

Challenges in decay rate change measurement in a Penning Trap . . . 19

II Contributed Oral **21**

Quantum computing with X- junction for 2D navigation of trapped ion qubits . . . 23

High-Harmonicity Planar Penning Traps for Single-Electron Qubits . . . 24

Induced charge coupling frequency of axial motion of two electrons trapped separately in 2-D planar Penning traps . . . 25

Photostability of isolated nucleotides under ultraviolet radiation . . . 26

Dynamical States of Driven Few-Ion Crystals . . . 27

Kinetic Monte Carlo Modelling of Recurrent Fluorescence in PAH Cations for the Delhi Penning Trap . . . 28

Non-Invasive Room-Temperature Detection of a Single Trapped Electron in VECC Penning Trap . . . 29

Identification and consolidation of decay hierarchy of statistical fragmentation network in aromatic molecules and their fragments . . . 30

III Contributed Abstracts **31**

Design, Development, and Characterization of a Dual Linear Paul Trap . . . 33

Formation of Nitrogen-Bearing PAHs: An Efficient UV-Induced Pathway in the Interstellar Medium . . . 34

Probing a New Formation Pathway for N-bearing PAHs in the Interstellar Medium Using a 22-Pole Ion Trap . . . 35

A 22-pole ion trap setup for astrophysically relevant reaction kinetic studies . . . 36

Delhi Penning Trap Setup For Experimental Study of Electron-Impact Ionization Cross-Section in Relativistic regime . . . 37

Design and Optimization of a Multilayer Axial Resonator for Ar+ Detection in the Delhi Penning Trap (DPT) . . . 38

From electrode asymmetry to octupole anharmonicity: quantum motional dynamics of a single ion in a Paul trap . . . 39

Quantum Beam-Splitter Cooling and Thermometry in Large Trapped-Ion Crystals . . . 40

Towards Paul trapping of single electron bubbles in liquid helium . . . 41

Analysis of an effective adiabaticity parameter to characterize ion temperatures in multipole radiofrequency ion traps . . . 42

Iodine anion photodetachment in a 16-pole ion trap . . . 43

Space-charge-limited Coulomb crystals in a 3D Paul trap: direct N-body simulation versus cold-fluid theory . . . 44

Quekit-SDK - An Indigenous SDK for virtual trapped-ion and quantum physics simulation . . . 45

Large associative ionization cross-section for low lying states of Li . . . 46

Electron Impact Ionization Cross Sections and Rate Coefficients for the CS_2 Molecule . . . 47

Longitudinally Polarized Electron-Induced Ionization of Palladium Atoms: A Relativistic Spin-Asymmetry Study . . . 48

Electron-impact total ionization cross sections for neutral Erythrulose $C_4H_8O_4$ . . . 49

K-LL Auger- Meitner emission in symmetric projectile ion- target molecule collision. . . . 50

Electron and Ion Radiation Processes on Astrophysical Ice Surfaces: Development of a New Experimental Facility at SINP, Kolkata, India . . . 51

Electron-induced x-ray emission from thick Pb and Pt targets: Experimental measurements and PENELOPE simulations . . . 52

Study of electron impact ionization and excitation cross sections of beryllium isoelectronic sequence . . . 53

Laboratory Simulation of Titan's Ionospheric Conditions . . . 54

Modelling Plasmon Excitations in Planar PAH Systems . . . 55

Fragmentation dynamics of exotic ionic species derived from the toluene cation under CID . . . 56

Pyridine under Electron-Impact and Multiphoton Ionisation: Estimation of Appearance Energies and Identification of Dissociation Pathways . . . 57

Appearance Energy of Benzonitrile Fragment Cations Under Low Energy Electron Impact . . . 58

Energy resolution and absolute efficiency calibration facility for Low-energy plasma sensor for Venus Mission . . . 59

In search of evidence of plasmon excitation in PAHs at low-energy electron impact . . . 60

Proposal for the Direct Measurement of the Zero-Point Energy . . . 61

Laser-Induced,Blackbody-Radiation-Assisted Rovibrational Cooling of Linear Triatomic Molecules . . . 62

Free-Induction-Decay Atomic Magnetometer with a MEMS Cesium Vapor Cell . . . 63

General Purpose, Modular and Customizable Integrated Data Acquisition and Control System (IDACS) For Charged Particle Instrumentation . . . 64

Characterization of a trapped ion platform: potential, micromotion, heating, and scattering . . . 65

Linewidth measurement of a home-built external cavity diode laser via self-heterodyne interferometry . . . 66

Part I

Invited Talks

Planar Trap Arrays for Quantum Information Processing and Simulation with two-dimensional Charged-Particle Crystals

M. Vogel[†]

GSI Helmholtzzentrum fuer Schwerionenforschung, 64291 Darmstadt, Germany

Synopsis Individually confined charged particles can be used as qubits, and their mutual interaction in arrays of traps can be taken as a means of simulating quantum systems or processing quantum information. I will introduce to the topic of such trap arrays and give a short account of endeavours in this field of research.

About thirty years ago, quantum information processing with confined ions was proposed by Cirac and Zoller, and scalability was regarded as a central aspect of such systems by DiVincenzo. In the years following that, a number of physical systems and methods have been proposed to realise and demonstrate the preparation of qubits based on confined charged particles such as ions or electrons, and to demonstrate the processing of quantum information via controlled gate operations. As part of this endeavour, the desire arose to work with systems in which each particle is confined separately and by use of static fields only. This has led, amongst others, to the proposition of two-dimensional arrays of planar Penning traps that confine a single ion or electron each, and to use the interaction between the charges as a means of communicating quantum information. Conventional 3D Penning traps can be transformed into 2D versions (see figure 1) that can be arranged in a plane and micro-fabricated on a planar chip.

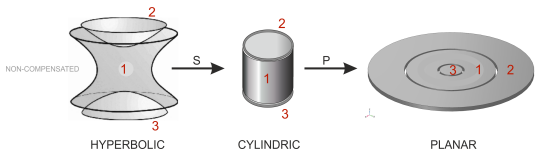

Figure 1. Genealogy of transformations leading to the planar Penning trap (prototypical case).

In the language of plasma physics, the resulting particle arrangements, either of many particles confined in a single trap or of individual particles confined in a multitude of traps, can qualify as charged-particle crystals, either ion Coulomb crystals or electron Wigner crystals in which the degree of particle-particle correlation is so high that only collective descriptions apply, and consequently the rate of communication allows for efficient processing. Similar systems had been proposed even earlier and in parallel also for other applications. A number of experimental endeavours have been undertaken and are currently being pursued, including one at IUAC. I will try to motivate the use of such trap arrays, show principles and examples of experimental realisations and discuss general features from the standpoint of an experimental physicist.

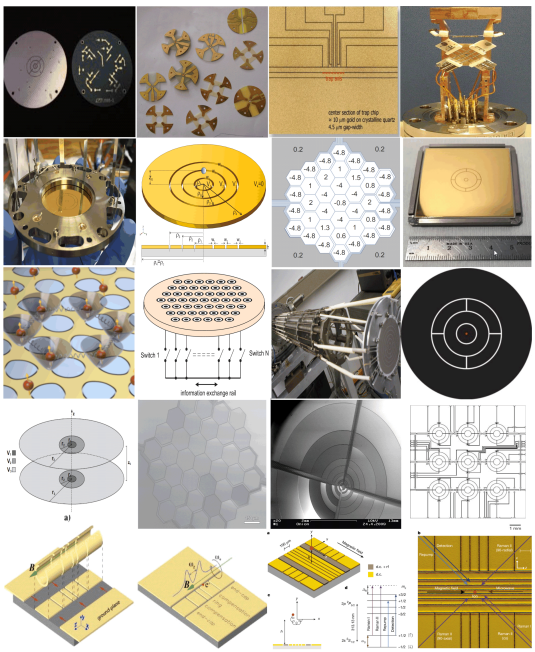

Figure 2. Collage of impressions from the world of planar Penning traps and their arrangement in the two-dimensional plane.

[†]E-mail: m.vogel@gsi.de

A Scalable 2D Planar Penning Trap Architecture for Trapped-Electron Quantum Computing

Sugam Kumar[1†], Kedar Mal[1], Veena C.P.[1], C.P. Safvan[1], W. Quint[2], Stefan Stahl[3], Irene Marzoli[4], Ferdinand Schmidt-Kaler[5], Jose Verdu Galiana[6] and M. Vogel[2]

[1]Inter-University Accelerator Centre, New Delhi 110067, India
[2]GSI Helmholtzzentrum für Schwerionenforschung, 64291 Darmstadt, Germany
[3]Stahl-Electronics, Kellerweg, Mettenheim, Germany
[4]Physics Division, School of Science and Technology, Università di Camerino, Italy
[5]Institute of Physics, Johannes Gutenberg University Mainz, Germany
[6]Department of Physics and Astronomy, University of Sussex, United Kingdom

Synopsis Planar Penning traps offer a route to quantum computing based on trapped electrons, combining long-lived spin states with microwave control and the absence of radio-frequency trapping fields [1, 2]. The main challenge is to move from a single micro-sized trap to a compact and scalable array while retaining a sufficiently harmonic potential and reliable detection of individual electrons.

We are developing a 2D array of micro-sized planar Penning traps for quantum computing with trapped electrons. The proposed trap consists of concentric planar electrodes with dimensions in the tens of micrometres and an inter-trap spacing of about 100 μm. The electrode geometry is being optimized to reduce anharmonicity of the axial potential, since amplitude-dependent frequency shifts can affect coherent control. Recent calculations of sub-millimetre planar traps show that finite electrode gaps have to be included at this scale and that a three-gap geometry is a suitable building block for a 2D array [1]. For the optimized micro-trap, axial frequencies in the few-GHz range are obtained with modest electrode voltages.

In the proposed quantum processor, the two spin states of each trapped electron form the logical qubit [2]. Microwave radiation is used to drive the electron-spin transition and implement single-qubit operations. The axial vibrational motion provides a common motional degree of freedom through which the Coulomb interaction between electrons can be used to generate two-qubit coupling [2]. Carrier and red- and blue-sideband transitions therefore provide a direct route to entangling operations, including a CNOT-type sequence. This approach avoids the laser systems normally required for trapped-ion quantum computing.

The experimental system will operate in a dilution refrigerator under a strong magnetic field. Electron motion will be detected through image currents using a high-Q resonant circuit, while spin states will be read out using the continuous Stern–Gerlach technique [2, 3]. A superconducting resonator and cryogenic HEMT amplifier provide low-noise detection. This work combines micro-trap design, cryogenic integration and microwave control towards a scalable 2D trapped-electron quantum processor.

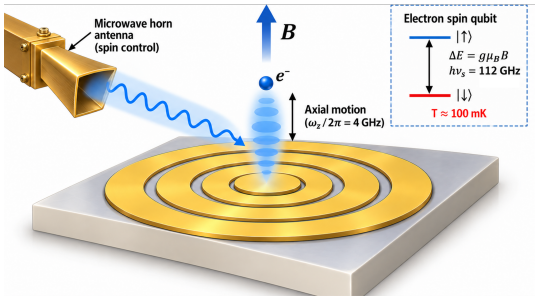

Figure 1. Schematic of a micro-sized planar Penning trap for trapped-electron quantum computing. A single electron is confined above the planar electrode array in a strong magnetic field. Microwave radiation from a horn antenna is used to control the electron spin, while the axial motional frequency is approximately 4GHz.

References

[1] S. Stahl *et al.* 2005 *Eur. Phys. J. D* **32** 139
[2] I. Marzoli *et al.* 2009 *J. Phys. B: At. Mol. Opt. Phys.* **42** 154010
[3] P. Bushev *et al.* 2008 *Eur. Phys. J. D* **50** 97

†E-mail: sugamkumar@gmail.com

Trapped ion quantum computing

Ferdinand Schmidt-Kaler [1†],

[1]QUANTUM, Institut für Physik, Johannes Gutenberg Universität Mainz, Germany

My talk introduces quantum computing with trapped ions and then focusses on the shuttle-base approach. I am discussing the compilers, which transform an incoming quantum circuit into a sequence of single and two-qubit gate operations and the shuttle operations on the trapped ion quantum register. I discuss specific advantages of different architectures and show how a versatile 3D sculpturing can be used to realize trapping structures, which realize such architectures. Finally, I sketch test cases which we have run on the quantum computer. This includes building blocks of quantum error correction, hybrid quantum/classical computation such as variational eigensolver and a machine learning process.

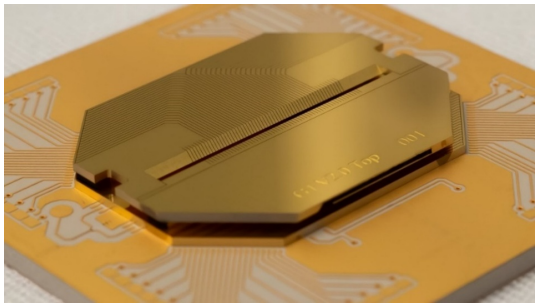

[†]E-mail: fsk@uni-mainz.de

Rack-assembled, high-uptime $^{171}Yb^{+}$ single-ion optical clock with systematic uncertainty below 2x10^{-17} and instability below 4x10^{-18}

A. Friedenauer[1], P. Thoumany[1], C. Tresp[1], D. Heinrich[1], D. S. Ritter[1] and J. Stuhler [1†]

[1] TOPTICA Photonics SE, Lochhamer Schlag 19, 82166 Graefelfing, Germany.

We present TOPTICA's optical frequency standard TOPTICLOCK. It is based on the $^{2}S_{1/2}$ (F=0) $-^{2}D_{3/2}$ (F=2) electric quadrupole (E2) transition at 435.5 nm of a single laser-cooled and trapped $^{171}Yb^{+}$ ion. All required subsystems are contained in two transportable 19"rack compartments. TOPTICLOCK was transported to the German National Metrology Institute (Physikalisch-Technische Bundesanstalt, PTB) and compared to a research-style Yb-ion optical frequency standard operating at the electric octupole (E3) transition at 467 nm. A frequency instability of 5x10$^{-15}/\sqrt{t}$ with no flickering or drift observed down to $<$ 4x10^{-18} and a total systematic uncertainty below 2x10^{-17} was demonstrated. In addition, the overall performance of the TOPTICLOCK was benchmarked by directly comparing it to another, fully independent Yb-ion optical frequency standard operating also at the E2 transition. An agreement between both systems with a total uncertainty well below 1e-17 was obtained.

[†]E-mail: juergen.stuhler@toptica.com

Quantum physics with trapped ions

Manoj Kumar Joshi [†]

[1]Singapore University of Technology and Design, Singapore

Trapped-ion systems provide a well-isolated environment for developing high-fidelity quantum technologies. Their individual qubit control, long coherence times, and ability to engineer long-range interactions mediated by light and phonons make them a powerful platform for next-generation quantum technologies. In this workshop, I will present recent results in quantum simulation on a trapped-ion quantum simulator. In particular, I will demonstrate how spin relaxation can be investigated in individually controlled, interacting ion chains. I will also discuss the technical challenges associated with scaling up such platforms and provide an outlook on future research directions with large-scale trapped-ion systems.

[†]E-mail: manoj_joshi@sutd.edu.sg

Seeking advantage in Quantum-Classical Machine Learning with trapped ion system

Manas Mukherjee [1†]

[1]Centre for Quantum Technologies,National University of Singapore.

Quantum technologies, specifically Quantum Computing (QC), represent a paradigm shift in computational power. However, the roadmap to utility is hindered by the inherent fragility of quantum states —a hurdle that makes scaling the industry's greatest challenge. To address this, we have developed a quantum-classical hybrid framework designed to push the boundaries of Quantum Machine Learning (QML). By leveraging the trapped-ion platform—noted for its superior coherence times and high gate fidelities—we have demonstrated that quantum classifiers can achieve over 98 % fidelity in supervised learning tasks using real-world datasets. While achieving parity with classical systems is a significant milestone, our current research pivots toward the ultimate goal: identifying the specific parameters and architectures where QML provides a definitive advantage over classical counterparts. Here, we will discuss detail of our findings across varied application contexts, highlighting the conditions under which quantum enhancement becomes a reality.

[†]E-mail: cqtmukhe@nus.edu.sg

Developing a high-fidelity calcium-ion quantum computer

S R Chanu[1,2†]

[1] Department of Physics, Indian Institute of Technology Kanpur, Kanpur, UP 208016, India. [2]Centre of Lasers and Photonics, Indian Institute of Technology Kanpur, Kanpur, UP 208016, India

Trapped-ion systems are among the leading platforms for scalable, fault-tolerant quantum computing because of their long coherence times, identical atomic qubits, and all-to-all connectivity. Our choice of calcium-40 (^{40}Ca+) and calcium-43 ($^{43}Ca^{+}$) offers distinct advantages, including accessible optical wavelengths compatible with diode laser technologies and clock transitions that are remarkably insensitive to magnetic field fluctuations. However, scaling these systems while maintaining gate errors below the fault-tolerance threshold remains a significant engineering and physics challenge. In this talk, we present our recent progress toward building a high-fidelity calcium ion quantum processor at the Indian Institute of Technology Kanpur. We will discuss advancements in Linear Blade electrode ion traps designed to suppress anomalous motional heating, alongside precision optical control techniques that minimize laser phase noise and crosstalk during single- and two-qubit Mølmer–Sørensen entangling gates. Furthermore, we will detail our strategies for fast, low-error state preparation and readout, as well as the integration of mid-circuit measurement and ion shuttling protocols essential for quantum error correction. Finally, we will highlight our plan to implement and demonstrate state-of-the-art gate fidelities and outline our roadmap toward fault-tolerant logical qubit operations.

[†]E-mail: sranjita@iitk.ac.in

Quantifying the rate for rare events using trapped ions

Akhil Ayyadevara[1], Anand Prakash[1], Shovan Dutta[1], Arun Paramekanti[2] and S. A. Rangwala[1†]

[1]Raman Research Institute, C. V. Raman Avenue, Sadashivanagar, Bangalore 560080, India
[2]Department of Physics, University of Toronto, 60 St. George Street, Toronto, Ontario, M5S 1A7 Canada

Synopsis We use the flipping rate of a five-ion pyramidal crystal inversion of laser cooled Ca ions to validate the Kramers-Langer theory.

Rare events are processes which occur on timescales which are far longer than the timescales intrinsic to the system under study. These are hard to study systematically since the statistics for such systems are hard to obtain under controlled circumstances. In thermal equilibrium, such rare events arise when thermal fluctuation cause the system to change state. The foundational theoretical work to understand such systems, was provided by Kramers [1] and generalized to multi-dimensional systems by Langer [2] and the overall framework for the rate of change of a system in a metastable state requires goes by the name of the Kramers-Langer theory. The testing of this theory requires a system close to thermal equilibrium, with a controllable energy landscape.

Laser cooled and trapped Ca ions, which self organise into a cluster, provide an ideal system to experimentally verify the theory [3, 4] . Laser cooled ions are close to thermal equilibrium, and the energy landscape is completely determined. The flip rate of the pyramid, between the equally probable up and down pyramid, as a function of a precisely controllable barrier height is then used to determine the agreement between the flip rates predicted by the Kramers-Langer formulation and the Molecular-Dynamics simulations with the experimentally determined theory parameters. The agreement is very close. This is then used to determine the temperature of the 5-ion pyramidal crystal [5]. It is also shown that permutation symmetry plays an important role in pyramidal inversion, which is experimentally demonstrated by breaking the permutation symmetry by working with isotopically mixed crystals. This work therefore demonstrates the power of simple mesoscopic atomic physics systems to extend far beyond the confines of the field.

References

[1] H. Kramers, Physica A (Amsterdam) **7**, 284 (1940)
[2] J. Langer, Ann. Phys. (N.Y.) **54**, 258 (1969)
[3] Anand Prakash *et al.* AIP Advances **16**, 075202 (2026)
[4] Akhil Ayyadevara *et al.* Phys. Rev. Res. **8**, L012066 (2026)
[5] Akhil Ayyadevara *et al.* Phys. Rev. Lett. **137**, 023002 (2026)

†E-mail: sarangwala@rri.res.in

HiThor@Spectrap - A Penning Trap to faciliate a Thorium Nuclear Clock

S Ringleb[1,2†], M Vogel[1], J Henning[1,3], Th Stöhlker[1,2]

[1]GSI Helmholtzzentrum fuer Schwerionenforschung GmbH 64291 Darmstadt, Germany
[2]Helmholtzinstitut Jena 07743 Jena, Germany
[3]Friedrich-Schiller-Universität Jena 07743 Jena, Germany

Synopsis We will present the basic idea of the thorium nuclear clock and describe the used Penning trap to capture the ions from an accelerator and prepare them for laser-ion interaction.

Highly-ionized-thorium clocks are ideal for tests of fundamental interactions since the ions are elementary quantum systems composed of only a few building blocks. Two cases of $^{229}Th^{q+}$ clocks excel. On the one hand, one-electron $^{229}Th^{89+}$ that combines two nuclear-clock transitions in the VUV with hyperfine IR atomic-clock transitions, and on the other hand fully ionized $^{229}Th^{90+}$ which constitutes the prototype of a nuclear clock, one without any electrons. [1] In the first state, the effect of nuclear hyperfine mixing is present which facilitates the excitation of the one electron from the ground state to the first isomeric state. One step to investigate the feasability of a nuclear clock is the storage of such ions in a Penning trap and measure the transition energy and lifetime of the isomeric state. Here, the transition energy is about 8.36 eV which can be driven by a UV-laser. To prepare the ions in a defined position, we have developed a Penning trap optimised to capture ions from an accelerator. This a accomplished by a set of deceleration stages and by a well-designed electronically compensated trap.

The transition energy and the lifetime are measured with laser excitation of the stored ions with subsequent measurement of the emitted photons from the relaxation process. To cover a large opening angle, we have decided to eliminate the ring electrode from our design and placed 16 silicon photo multipliers (SiPM) in the central plane of the trap. This design has been verified to allow a good harmonicity of the trap but comes along with no orthogonality. Upon ion capture, the ions will be cooled fast using resistive cooling [2]. In this context, we have calculated the axial frequency dependence of stored ions depending on their kinetic energy. We have found the ion frequency spread to be less than the typical width of a normal conducting resonant circuit which is hence suitable to cool all captured ions fast and at once. This will allow efficient ion confinmement in the trap centre.

We will present the thorium nuclear clock experiment (ERC Advanced Research Grant "HiThor") and the Penning trap as a part of this project. We will give some insight into the envisaged ion storage techniques and laser measurements.

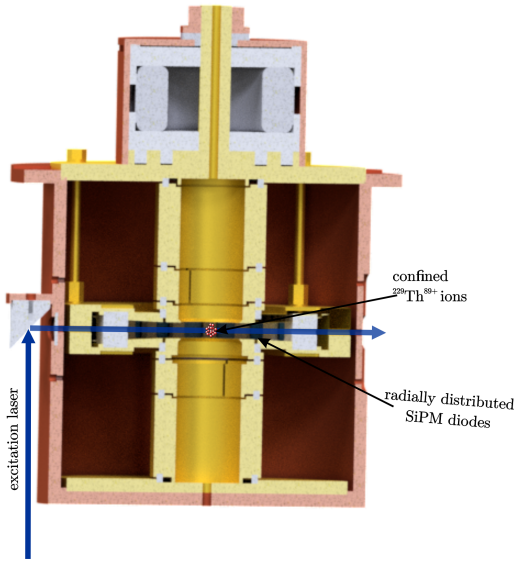

Figure 1. HiThor Penning trap consisting of six electrodes for electronic compensation. The eliminated ring electrode is replaced with a set of 16 SiPM to measure emmitted photons.

References

[1] Brandau C *et al.* 2026 arXiv:2608.08133v1 [physics.atom-ph]
[2] Kiffer M *et al.* 2024 *J. Appl. Phys.* **136** 184901

†E-mail: stefan.ringleb@hi-jena.gsi.de

Trapped Ion based Optical Atomic Clock: A Possible Way of Redefining SI Second

Subhasis Panja †

CSIR-National Physical Laboratory, Dr. K S Krishnan Marg, New Delhi 110012, India
Academy of Scientific & Innovative Research, Ghaziabad 201002, India

Synopsis We report progress at CSIR-NPL towards a single-ion $^{171}Yb^{+}$ optical clock based on the 435 nm electric-quadrupole transition. The ion is trapped in an rf Paul trap under ultra-high vacuum and laser cooled at 369.5 nm with 935 nm and 760 nm repump lasers. The clock laser is narrowed by locking to an ultra-low-expansion Fabry–Pérot cavity (finesse 50000, FSR 1.5 GHz). Optical clocks may enable a redefinition of the SI second.

The present definition of time or frequency is based on a microwave transition of laser-cooled caesium atoms. The variance of the measurement, the "Allan deviation", is inversely proportional to the resonance frequency, so an optical frequency standard with a resonance frequency of a few hundred THz can be two to three orders of magnitude more accurate than a microwave frequency standard [1]. It is expected that the SI unit of time will be redefined with an optical clock, based either on the atomic transition of ultra-cold atoms confined in optical lattices or on a single ion trapped in a radio-frequency ion trap and laser cooled [2,3].

At CSIR-NPL we are working towards building an optical atomic clock based on the quadrupole transition of a single ytterbium ion, stored in a Paul trap inside an ultra-high vacuum. The ion confined within the rf trap will be cooled to micro-Kelvin temperature using laser cooling to restrict its motion to the Lamb–Dicke regime. The strong transition at 369.5 nm will be used for laser cooling. However, in this case the excited state decays to two different metastable states, so two repump lasers at 935 nm and 760 nm will be used to deplete the long-lived metastable states and achieve closed-loop laser cooling. Hence three lasers at different frequencies are needed for laser cooling alone (Fig. 1). For clock operation we need to measure the transition at 435 nm, which has a natural linewidth of a few Hz. However, light from a typical extended-cavity diode laser has a linewidth of a few tens of kHz, and it is not possible to measure such a narrow spectrum with a laser of kHz bandwidth. For line narrowing, the laser will be locked to a highly stabilised Fabry–Pérot cavity. The cavity, of finesse 50000 and free spectral range 1.5 GHz, will be made of ultra-low-expansion material which has a zero expansion coefficient at room temperature. The present article describes activities and progress towards developing the optical atomic clock at CSIR-NPL.

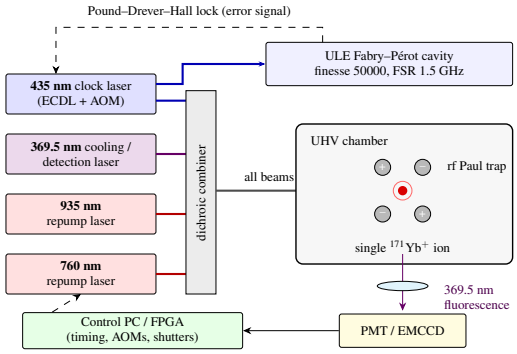

Figure 1. Schematic of the experimental setup for a single-ion $^{171}Yb^{+}$ optical clock. The 369.5 nm cooling, 935 nm and 760 nm repump beams and the 435 nm clock beam are overlapped on a single ion in an rf Paul trap in UHV. The clock laser is pre-stabilised to an ULE cavity; 369.5 nm fluorescence is detected with a PMT or EMCCD.

References

[1] Sharma L, Rathore H, Utreja S, Neelam, Roy A, De S and Panja S 2020 *MAPAN–J. Metrol. Soc. India* **35** 531
[2] Aeppli A, Kim K, Warfield W, Safronova M S and Ye J 2024 *Phys. Rev. Lett.* **133** 023401
[3] BACON Collaboration 2026 *Phys. Rev. Lett.* **137** 033201

†E-mail: panjas.nplindia@csir.res.in

Zero-Point Energy of the Electron in a Penning Trap by Photo-Detachment Laser Spectroscopy

Sugam Kumar[1], S. Fritzsche[2], W. Quint[3†], and M. Vogel[3]

[1]Inter-University Accelerator Centre, New Delhi 110067, India
[2]Helmholtz-Institut Jena, 07743 Jena, Germany
[3]GSI Helmholtzzentrum für Schwerionenforschung, 64291 Darmstadt, Germany

Synopsis We discuss the confinement of an electron in a Penning trap as the realisation of a quantum-mechanical harmonic oscillator. In such a situation, the non-zero ground-state energy of the electron in the confining electric and magnetic fields of the trap (as compared to the classical zero of the energy of a free electron) can be directly measured with high precision in photo-detachment spectroscopy of confined negative atomic ions such as H^-. We detail a concrete implementation of such a measurement and discuss its implications.

In stark contrast to classical physics where confined particles can have exactly zero energy, quantum theory exhibits a finite zero-point energy (ZPE) that represents the lowest possible energy state of a system. This energy is an inherent feature of quantum systems, arising from the Heisenberg uncertainty principle. One significant remark comes from Feynman's lectures: 'The vacuum is not empty. It is filled with fluctuating fields. The ZPE is the lowest energy state of these quantum fluctuations, and its consequences are observable, as in the Casimir effect.' It is important to note that the Casimir effect refers to the ZPE of the pure electromagnetic field. However, the ZPE associated with a massive quantum-mechanical harmonic oscillator such as a confined particle remains largely unexplored experimentally.

We propose to directly measure the absolute value of the ZPE of a confined particle with high precision by laser photo-detachment spectroscopy of negative hydrogen ions H^- that are confined by the electric and magnetic fields of a Penning trap. The photodetached electron in the trap behaves as a quantum mechanical harmonic oscillator with energy levels $(N + 1/2)\,\hbar\omega$, where the electron's motional frequencies ω can be controlled by adjusting the electric and magnetic field strengths. In the ground state of the cyclotron motion, which gives by far the largest contribution, the ZPE $\hbar\omega^+/2$ of the confined electron leads to a measurable shift in the photodetachment threshold compared to the free-particle case.

This shift can be measured with high precision by laser photo-detachment spectroscopy. The photon energy $h\nu$ required to detach the electron is given by the electron affinity E_a = 0.754195(19) eV of the H^- anion. However, when the detached electron is not free to go to the continuum, but remains confined for example in a Penning trap, where it occupies the quantum-mechanical ground state of oscillation in the trap, the ZPE $\hbar\omega^+/2$ of the confined electron adds to this energy threshold, i.e. $h\nu = E_a + \hbar\omega^+/2$. A measurement of the photo-detachment cross section as a function of photon energy in the trap yields the threshold value $h\nu = E_a + \hbar\omega^+/2$. Subtracting the well-known free-particle value E_a provides a direct measurement of the ground-state ZPE $\hbar\omega^+/2$ [1]. (see Fig. 1).

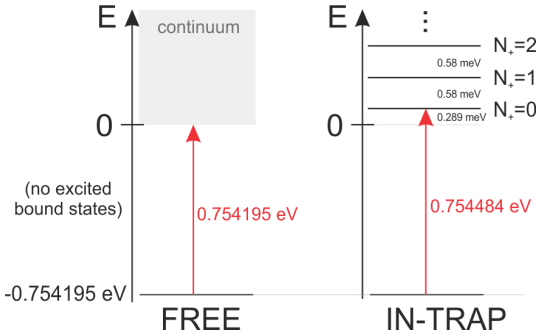

Figure 1. Energy level scheme for photodetachment laser spectroscopy of negative atomic hydrogen H^- in free space (left) and in a Penning trap (right).

References

[1] S. Kumar *et al.* 2025 *J. Phys. B: At. Mol. Opt. Phys.* **58** 245002

†E-mail: w.quint@gsi.de

Near threshold statistical dissociation of quinoline cations using action spectroscopy in cryogenic storage

Umesh Kadhane[1†]

[1]Atomic and Molecular Physics Laboratory, Indian Institute of Space Science and Technology, Thiruvananthapuram, Kerala 695547, India

Synopsis Quinoline, a polycyclic aromatic nitrogen heterocycle (PANH), is of interest in astrophysical chemistry due to its potential role in the formation of complex organic molecules. This study explores the photodissociation dynamics of quinoline cations through experiments conducted at the cryogenic ion storage ring DESIREE, Stockholm University. The observed wavelength-dependent decay rates, possible two-photon processes, and signatures of recurrent fluorescence challenge established interpretations and raise fundamental questions about conventional RRKM theory and the underlying dissociation mechanisms.

Polycyclic aromatic nitrogen heterocycles (PANHs), and quinoline in particular, represent very important type of aromatics in astrophysical chemistry. The detection of Aromatic Infrared Bands (AIBs), attributed to polycyclic aromatic hydrocarbons (PAHs) and their clusters, together with the confirmed identification of nitrogen-containing aromatics including benzonitrile, cyanonaphthalene, cyanopyrene, and cyanocoronene, demonstrates their abundance and widespread distribution throughout the interstellar medium (ISM). Current hypotheses on the origin of these cyclic species highlight a combined association and dissociation processes as central mechanisms. A critical stage in chemical evolution involves the rapid fragmentation of molecules, generating reactive intermediates that drive subsequent pathways. Protoplanetary discs provide a key example: energetic radiation—ultraviolet, X-rays, and cosmic rays—penetrates to varying depths depending on opacity and radiation type, initiating complex chemistry. Likewise, high-energy charged particles and solar UV radiation catalyze reactions in planetary atmospheres, such as Titan, ultimately leading to the formation of complex organics.

Given the astronomical relevance of PANHs, their statistical dissociation dynamics warrant detailed investigation. Quinoline has therefore been the subject of PEPICO/VMI studies over the past five years, with particular attention to dissociation channels involving the loss of HCN, HNC, C_2H_2, and $HCNH$—species that play crucial roles in the evolution of larger organics in astrophysical environments [1, 2]. Structural calculations combined with RRKM modeling have been employed to complement these experiments. However, the substantial kinetic shift inherent to conventional approaches hindered validation of RRKM predictions. To address this, experiments on quinoline cations were conducted at cryogenic double ion storage ring DESIREE at Stockholm University, designed to minimize kinetic-shift effects and probe statistical decay near threshold.

Unexpectedly, the results diverged sharply from expectations and established understanding. First, the observed decay rates as a function of excitation wavelength directly challenge several well-established findings. Second, if the decay proceeds via two-photon processes, this implies highly specific and complex excited-state dynamics in quinoline cations. Third, the evolution of decay rates across laser shot sequences revealed signatures of recurrent fluorescence. Consequently, an experiment originally intended to confirm the applicability of conventional RRKM theory now raises fundamental questions about the established mechanisms of quinoline ion photodissociation.

References

[1] Arun S, Ramanathan K, Selvaraj M, Cautero M, Richter R, Pal N, Chiarinelli J, Bolognesi P, Avaldi L, Vinitha MV, Jureddy CS, Kadhane UR. 2023 *J. Chem. Phys.* **159** 104308

[2] Ramanathan K, Arun S, Bouwman J, Avaldi L, Vinitha MV, Bolognesi P, Richter R, Kadhane UR. 2022 *J. Chem. Phys.* **157** 064303

†E-mail: umeshk@iist.ac.in

Quantum Sensing with Neutral Atoms and High-Precision Diode Lasers

Bodhaditya Santra[1,2†]

[1]Department of Physics, Indian Institute of Technology Delhi, New Delhi 110016, India
[2]Prenishq Pvt. Ltd., Synergy Building, TBIU Complex, IIT Delhi, New Delhi 110016, India

Synopsis Our work is focused on developing compact laser systems and cold-atom platforms based on laser cooled ^{133}Cs atoms for precision quantum sensing. Our research integrates the development of accessible external cavity diode lasers and embedded frequency stabilization with investigations of cold-atom dynamics, collisional losses, detection noise and photon-mediated collective effects in magneto-optical traps. These advances provide the foundation for developing transportable cold-atom gravimeters and optical magnetometers with high sensitivity and stability for precision measurements of gravitational and magnetic fields in field applications.

Laser-cooled atomic ensembles serve as foun dational platforms for next-generation quantum technologies, enabling breakthroughs in precision spectroscopy, quantum computing, and quantum sensing. Translating their potential into practi cal applications requires compact, robust opti cal hardware and a quantitative understanding of atomic dynamics and detection noise. Our work is focused on laser-cooled ^{133}Cs ensembles in Magneto-Optical Trap (MOT), bridging founda tional atomic physics with field-deployable quan tum instrumentation. On the hardware and instrumentation front, we have developed accessible, high-performance optical subsystems tailored for cold-atom exper iments. We designed and developed a compact external-cavity diode laser (ECDL) in the Lit trow configuration, operating at the caesium D2 line. Built using readily available components, it features a custom collimation mount with a 3× wider adjustment range than commercial hold ers. The laser enables direct cooling and trap ping of ^{133}Cs atoms in a MOT without requir ing tapered amplifiers or injection locking [1]. To achieve long-term frequency stability, we de veloped an embedded digital PID locking sys tem based on an STM32 microcontroller, using dichroic atomic vapour laser locking (DAVLL) and a custom 150 V piezo driver. The system provides a 6 GHz mode-hop-free tuning range and reduces the laser linewidth to 93±2 kHz [2], enabling reliable trapping of ~ 1.5 × 106 ^{133}Cs atoms [3]. Alongside hardware development, we inves tigate collisional losses and collective effects in cold-atom clouds. We characterized light assisted collisions during fluorescence imaging to extract loss coefficients, reconstruct atom num bers and quantify detection noise and readout fidelity [4]. We also studied photon-mediated interactions and nonequilibrium dynamics in a Cs MOT through spatial density profiles, cloud width fluctuations and density correlations at dif ferent laser detunings. Using a generalized Lane Emden model and spectral correlation analy sis, we identified detuning-dependent interac tion regimes and scale-dependent density corre lations [5]. Building directly upon these validated hard ware platforms and noise-characterization frame works, our ongoing research is focused on trans lating cold-atom ensembles into practical, high precision quantum sensors. Specifically, we are developing cold-atom gravimeters and op tical magnetometers that leverage our compact laser architectures, embedded stabilization sys tems, and loss-compensated detection protocols to achieve high sensitivity and operational stabil ity for geophysical and navigation applications.

References

[1] Singh N *et al.* 2025 *J. Mod. Opt.* **72** 2487894
[2] Singh D *et al.* 2025 *Rev. Sci. Instrum.* **96** 073001
[3] Kamalkant *et al.* 2026 *Rev. Sci. Instrum.* **97** 063202
[4] Yadav P, Singh N and Santra B 2026 *J. Phys. B: At. Mol. Opt. Phys.* **59** 215301
[5] Ghosh A *et al.* 2026 *Eur. Phys. J. D* **80** 138

†E-mail: bsantra@physics.iitd.ac.in

Detecting Trapped Atoms with Minimal Disturbance: Real-Time Readout through Spin Noise

Saptarishi Chaudhuri [†]

[1]Light and Matter Physics, Raman Research Institute, Bengaluru, India

Detecting trapped atoms while preserving their dynamics is a central challenge in quantum science. Conventional fluorescence and absorption measurements obtain information through light scattering, which can disturb the atomic sample. This talk will explore an alternative route: using optically measured spin fluctuations to reveal local atomic density with minimal perturbation. Drawing particularly on our work published in Applied Physics Letters 127, 044004 (2025), I will present Raman-driven spin noise spectroscopy as a practical probe of trapped cold atoms. The method combines two coherent Raman fields that couple neighbouring Zeeman states with a tightly focused, far-detuned optical probe. Detecting fluctuations in the probe's Faraday rotation provides a spatially selective signal of the driven atomic spin coherence. I will discuss its experimental implementation in cold potassium ensembles, the dependence of the signal on trapping and loading conditions, and the reconstruction of local density profiles. Comparison with fluorescence-based profiles provides a benchmark, while direct local probing offers particular advantages for clouds without spherical symmetry. The talk will also examine the prospects enabled by MHz rate data acquisition for following atomic dynamics, alongside connections to spin correlation measurements and precision magnetometry. Finally, I will discuss how minimally perturbative optical detection could support neutral-atom quantum computing and quantum sensing, distinguishing demonstrated ensemble-density measurements from future qubit-readout applications.

[†]E-mail: srishic@rri.res.in

Observation of spontaneous N-bearing PAH formation using an ion trap: A new formation pathway in the interstellar medium

Siddhartha S. Payra and G. Aravind[†]

Department of Physics, Indian Institute of Technology Madras, Chennai-600036, India

Synopsis We present an ion-neutral kinetic study of the reaction between pyrimidine cations and acetylene utilizing a 22-pole RF ion trap apparatus. This approach enables the investigation of sequential ion-molecule reactions under conditions that closely mimic those found in space, thereby providing critical experimental constraints for astrochemical models.

Nitrogen-bearing polycyclic aromatic hydrocarbons (N-PAHs) are key precursors to complex organic molecules in both the interstellar medium and the nitrogen-rich planetary atmospheres. Despite the recent detections of nitrogen-functionalized astromolecules, their formation pathways remain an open question. The discrepancies between their predicted and observed abundances point to unknown mechanisms such as ion-molecule reactions that govern their evolution in the astrophysical environments. Employing an ion trap technique (schematic of the experimental setup shown in Fig. 1 [1, 2]) in conjunction with electronic structure calculations, we unravel multiple barrier-less reactions between gas-phase pyrimidine cations ($C_4H_4N_2^+$) and acetylene (C_2H_2). The second-order rate coefficient for the first acetylene addition was determined to be $(1.3 \pm 0.3) \times 10^{-10}$ cm^3 s^{-1}. Subsequent addition of a second acetylene molecule proceeds with a rate coefficient of $(2.2 \pm 0.9) \times 10^{-12}$ cm^3 s^{-1}, yielding a hitherto unreported endocyclic N-PAH cation ($C_8H_7N_2^+$), through an exothermic reaction pathway with $\Delta H = -2.73$ eV. The calculated infrared absorption spectrum of this final product, particularly the C=C stretching band, appeared at 6.16 μm, which is in close agreement with the 6.2 μm emission band observed in the interstellar infrared emission spectrum. This support the inclusion of N-PAHs in the astrochemical models aimed at explaining the origin of the 6.2 μm interstellar emission feature [3]. The present measurements on reactions involving a double-nitrogen substituted aromatic heterocycle have implications to the astrochemistry of both the Titan's atmosphere and the interstellar medium.

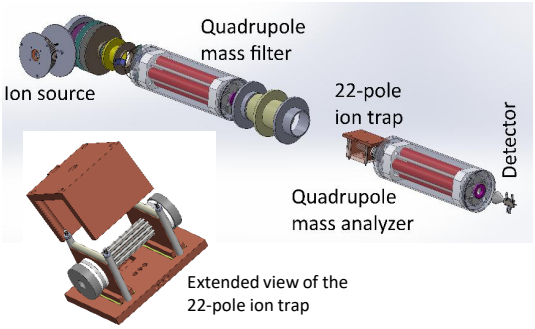

Figure 1. Schematic drawing of the modified 22-pole radio frequency ion trap setup. The ions are produced between the first two plates of the ion guide by electron impact ionization and repelled towards the QMS-1. Mass-selected ions are injected into the 22-pole trap. The trap is equipped with neutral and pulsed buffer gas input ports. A neutral density measurement gauge (Pfeiffer CMR 375) is also connected to the trap volume. After a specified trapping time, the ions are mass-analyzed by QMS-2 and counted in the CEM detector.

References

[1] Siddhartha S P *et al.* 2026 *ApJ* **1008** 212
[2] Nihar R B *et al.* 2024 *RSI* **95** 013201
[3] Sloan G C *et al.* 2003 *ApJS* **147** 379

[†]E-mail: garavind@iitm.ac.in

Effect of imperfections on the thermometry of ions stored in a 16-pole radiofrequency ion trap

S. Sunil Kumar[†], Vallari Kurdukar, and Pragya Nandan

IISER Tirupati, Durgiperi, Venkatagiri Road – 517619, India

Synopsis Multipole radiofrequency ion traps such as 22-pole and 16-pole ion traps are widely used for low-temperature studies relevant to laboratory astrophysics and astrochemstry, where the traps are cooled down to 4–100 K to simulate the interstellar medium (ISM). With the help of buffer-gas cooling, temperatures of the ions can be brought down to close to the buffer gas temperature after sufficient number of collisions. The temperature of the ions has been found to be always higher than the buffer-gas temperature due to a phenomenon called radiofrequency heating. In this study, we demonstrate that even a very small displacement ($\sim 50\,\mu$m) of the electrode position can cause substantial additional RF heating beyond what would occur in an ideal ion trap.

Multipole radiofrequency ion traps such as 22-pole or 16-pole traps are widely used for low-temperature studies such as spectroscopy of molecular ions in the ISM conditions and for measuring ion-molecular reaction rate coefficients as a function of temperatures relevant to astrophysical environments [1]. The ions are cryogenically cooled by lowering the temperature of the traps using a closed-cycle liquid-helium cryostat, and thermalized via collisional energy exchange with a buffer gas, typically helium.

A 22-pole or a 16-pole ion trap provides a relatively large field-free central region in which trapped ions undergo frequent collisions with helium buffer-gas atoms. As ions approach the radiofrequency (RF) electrodes, they experience the rapidly oscillating RF electric field [2]. RF-driven ion motion, coupled with buffer-gas collisions, can lead to RF heating and consequently to an ion translational temperature higher than that of the buffer gas. In this work, we investigate how small geometric imperfections in the fabrication of multipole ion traps influence the ion temperature.

We consider two trap geometries—a 16-pole and a 16-wire ion trap—with the same inscribed radius and hence the same nominal trapping volume. Both traps are operated at identical RF amplitudes and frequencies, and ions with $m/q = 17$ u (corresponding to OH^-) are simulated. Ions are generated within the trap and tracked for 25 ms. Their translational temperature is determined from the ion speed distributions, which are fitted to a Maxwell–Boltzmann distribution. The ions reach thermal equilibrium within approximately 10 ms; the reported temperature is therefore obtained by averaging the fitted temperatures over 10–20 ms.

Figure 1 shows the resulting ion temperature as a function of buffer-gas temperature for ideal 16-pole and 16-wire traps. For comparison, results are also presented for traps in which the alternate set of RF electrodes is displaced by $50\,\mu$m, representing a small geometric fabrication imperfection. The comparison reveals the sensitivity of ion heating to realistic deviations from the ideal trap geometry.

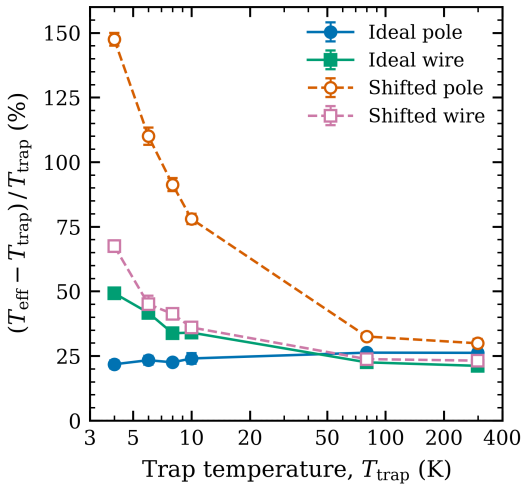

Figure 1. Percentage deviation of ion temperature in ideal and shifted 16-pole and 16-wire ion traps.

References

[1] Gerlich D 1992 *Advances in Chemical Physics* 1–176

[2] Asvany O and Schlemmer S 2009 *Int. J. Mass Spectrom.* **279** 147–155

[†]E-mail: sunil@iisertirupati.ac.in

Challenges in decay rate change measurement in a Penning Trap

Parnika Das[1,2†], Arindam Kr. Sikdar[1,2], Joydip Nandi[1], N. Chaddha[1,2],A. Ray[1*,2*(Ex)]

[1]Variable Energy Cyclotron Centre, 1/AF, Bidhannagar, Kolkata, INDIA
[2]Homi Bhabha National Institute, Anushaktinagar, Mumbai, Maharashtra, INDIA
[3]Delta Q, IMJ Institute of Research, Moodlakatte, Karnataka, INDIA

Synopsis The wide range of applications of nuclear science and technology are based the consideration that decay rate of a radioactive element is constant. Yet, continued experimental efforts have been made in search of conditions which would change the decay rate and questioned the accuracy of this "natural clock". Reported results show that the variation in decay rate in different terrestrial environment is ~ 1 %. However, dramatic change in decay rate has been observed in Storage ring experiments where extreme environment could be created. It is expected that tailored environmental conditions can be created in a Penning Trap by storing electron capturing nuclei in different charge state and substantial effects in decay rates will be observed. Efforts at VECC and at different labs and challenges in conducting such experiments will be discussed.

Among the different types of nuclear decay processes, electron capture by the nucleus is most susceptible to the surrounding environment. Since,^{7}Be is the lightest radioactive nucleiwhich decays via electron capture process, it is considered most susceptible. So, numerous studies have been performed and decay rate of ^{7}Be has been measured placing in different host media. In certain host lattice environment, where compression is not substantial, it is observed that the decay rate is directly proportional to the number of electrons in the 2s orbital of decaying ^{7}Be [2]. Number of 2s electrons in the 2s orbital (ns) of ^{7}Be, in a particular host media can be determined using density functional calculation [1].In Fig. 1, relation of (ns) with measured decay rate of ^{7}Be is shown. Qualitatively, loss of electrons from 2s orbital of ^{7}Be in a host medium due to hybridization can be considered as an effective ionization resulting reduction in electron density at the nucleus leading to change in decay rate. However, quantitative determination of decay rate change in a host medium is based on number of 2s electrons which is obtained from model dependent calculations.

In a storage-ring experiment, ionisation dramatically reduced the half-life from 41.6 billion years for neutral ^{1}87Re to about 33 years for fully ionized ^{1}87Re^{7}5+, demonstrating the profound influence of the atomic-electron environment on radioactive decay [3]. Such direct effect could be observed in a storage ring as an extreme condition of ionizing the decaying radioactive atoms could be achieved.

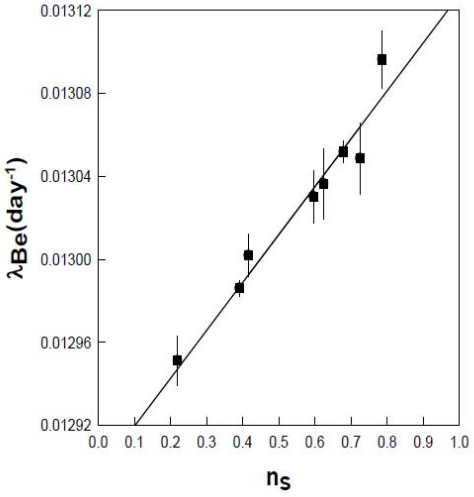

Figure 1. Decay Rate versus number of 2s electrons of 7Be

It is expected that such dramatic effects in ^{7}Be will be observed from measurement of ^{7}Be in different charge state in a Penning Trap. Exper imental setups for such measurements are being made at VECC and other labs [4]. Challenges in performing such experiments will be discussed.

References

[1] Andersen, O. K. *et al.* 1986 *Phys. Rev. B 34, 5253*
[2] P. Das *et al.* 2008 *Phys. Rev. C 71, 025801.*
[3] Bosch, F. *et al.* 2015 *Phys. Rev. Lett 77. 5190* **114** 162501
[4] https:/koethgroup.umd.edu/curie/

†E-mail: parnika@vecc.gov.in

Part II

Contributed Oral

Quantum computing with X- junction for 2D navigation of trapped ion qubits

S. Mohandas[†], A. Conta, J. C. Müller, C. M. Karres, and F. Schmidt- Kaler[†]

QUANTUM, Institute of Physics, 55128 Mainz, Germany

Synopsis At JGU Mainz, we are advancing scalable trapped-ion quantum computing by engineering precise ion transport across a segmented X-junction trap fabricated via Selective Laser Etching, using optimized voltage waveforms that minimize motional excitation during shuttling. The contribution covers the experimental setup, ground-state cooling, and junction-crossing benchmarks, demonstrating progress toward a scalable 2D architecture.

Trapped-ion quantum processors are currently transitioning from proof-of-concept laboratory experiments to robust, scalable, and user-ready devices. A critical requirement for large-scale computation, particularly within a Quantum Charge-Coupled Device (QCCD) architecture, is the ability to dynamically shuttle ions through multi-zone, micro-structured trap arrays. Leveraging advanced trapped ion control electronics, our team at Johannes Gutenberg University Mainz (JGU) is refining the reliable transport of ion crystals across complex trap junctions.

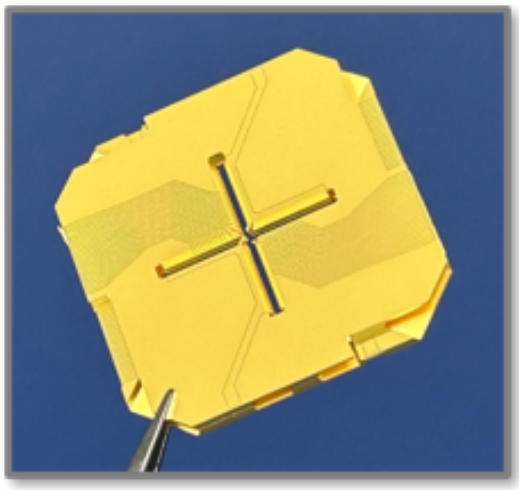

Figure 1. X-Junction ion trap with mutually perpendicular linear trapping segments. DC and RF tracks are also visible.

We utilize a segmented X-trap which is fabricated in our own clean room via Selective Laser Etching (SLE). Fully sculptured trap geometry has been meticulously engineered and scaled down to optimize radiofrequency (RF) requirements, mitigate anomalous heating, and minimize stray capacitance. The design features a central X-junction equipped with a split bridge to facilitate highly controlled transport. The voltage protocols driving this transport are generated using a recently developed numerical toolchain tailored for fast, low-excitation ion shuttling in segmented trap [1]. Based on a precise electrostatic model of our trap electrode geometry, this framework combines an electrostatic field solver with efficient unconstrained optimization and dynamical simulations of ion motion. It computes time-dependent voltage waveforms that realize prescribed transport trajectories across the junction while strictly adhering to real-world experimental constraints.

Here, I describe the experimental setup in detail. Moreover, I sketch the sequence comprising initial ground-state preparation via sideband cooling, followed by the transport of an ion crystal across the X-junction to benchmark the performance of both the SLE trap and the computed waveforms. Important characterizations include the measurement of the motional excitation per round trip. The X-trap will eventually serve to distribute qubit entanglement in a scalable 2D quantum computing architecture.

References

[1] A. Conta, S. Bogino, F. Köhncke, F. Schmidt-Kaler, and U. G. Poschinger, "Toolchain for shuttling trapped-ion qubits in segmented traps," *AVS Quantum Science*, vol. 8, no. 2, 2026.

[†]E-mail: smohanda@uni-mainz.de
[†]E-mail: fsk@uni-mainz.de

High-Harmonicity Planar Penning Traps for Single-Electron Qubits

Kedar Mal[1,2†], A.N. Agnihotri[1], Sugam Kumar[2], C.P. Safvan[2], W. Quint[3] and M. Vogel[3]

[1]Department of Physics, Indian Institute of Technology Delhi, New Delhi, 110016, India

[2]Inter-University Accelerator Centre, New Delhi 110067, India

[3]GSI Helmholtzzentrum für Schwerionenforschung, 64291 Darmstadt, Germany

Synopsis Planar Penning traps provide a promising platform for the confinement and control of single electrons, with potential applications in quantum information processing and precision measurements. For such applications, the anharmonicity of the trapping potential must be minimized to suppress unwanted frequency shifts and nonlinear coupling between motional modes. Achieving a highly harmonic confinement while maintaining a compact planar geometry is therefore a key challenge in the design of single-electron traps.

We investigate sub-millimetre planar Penning traps for highly harmonic confinement, essential for single-electron qubits in quantum information processing. Extending the treatment of larger planar traps [1], we show that finite electrode gaps become significant at the sub-millimetre scale and must be included in realistic designs. We optimize electrode geometries and voltages for harmonic confinement while minimizing the axial frequency shift Δf_z in three configurations: mirror-image, covered, and three-gap traps (see Fig. 1). These configurations can serve as building blocks for 2D trap arrays, with the three-gap trap attractive for future scalable implementations. For this configuration, we evaluate gap-potential models [2] by benchmarking their predictions against finite-element simulations. The optimized parameters and comparisons are summarized in Table 1 [3].

Table 1. Optimized three-gap trap parameters for different gap-potential models and finite-element simulation at $V_0 = -0.3591$ V, $f_z = 4$ GHz, and $\rho_1 = 10$ μm. Δf_z is in Hz.

Param.	Linear	Cubic	Corner	Sim.
ρ_3, (μm)	83.662	82.179	81.983	63.934
z_0 (μm)	13.714	13.592	13.575	12.490
V_1 (V)	9.573	9.397	9.373	7.180
V_2 (V)	9.807	9.629	9.606	7.374
V_3 (V)	26.841	27.069	27.102	38.252
a_2	0.0	0.0	0.0	$\sim 10^{-10}$
a_3	0.0	0.0	0.0	0.0
a_4	0.0	0.0	0.0	$\sim 10^{-9}$
a_5	0.0	0.0	0.0	0.0
a_6	-0.0043	-0.0044	-0.0044	-0.0079
Δf_z@4 K	0.731	0.750	0.752	1.3

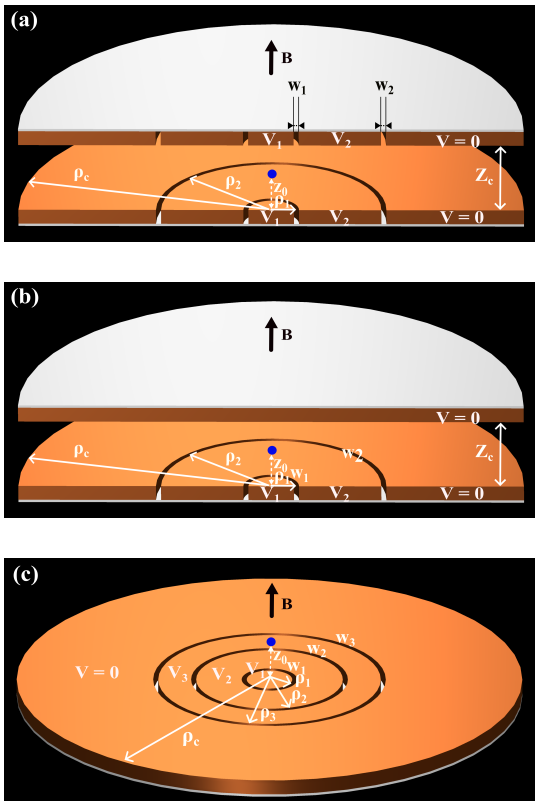

Figure 1. Schematic of the electrode structures of (a) a mirror-image trap, (b) a covered trap, and (c) a three-gap planar Penning trap. A stored electron is indicated at the centre of the trap, at a distance z_0 above the plane of the electrodes.

References

[1] J. Goldman *et al.* 2010 *Phys. Rev. A.* **81** 052335

[2] Farrar K 2002 *Nucl. Instrum. Methods Phys. Res. A* **485** 780

[3] K. Mal *et al.* 2026 *arXiv:2608.17984* **2608.17984**

†E-mail: kedarmaljangirphy@gmail.com

Induced charge coupling frequency of axial motion of two electrons trapped separately in 2-D planar Penning traps

Geetu Narang[1†], Manuel Vogel[2], Wolfgang Quint[2], Vicky Budhiraja[3] and Sugam Kumar[4]

[1]Department of Physics, Panjab University, Chandigarh, 160015, India
[2]GSI Helmholtzzentrum für Schwerionenforschung, Planckstraße 1, Darmstadt, 64291, Germany
[3]QUTE Electronics, 33/B/4/9, Vasant Kunj, New Delhi, 110070, India
[4]Inter-University Accelerator Centre, New Delhi, 110067, India.

Synopsis We present a theoretical framework for evaluating the interaction frequency of two charged particles confined in 2 D planar Penning traps. The interaction frequency is evaluated in terms of the capacitance of the planar traps along with the wire connecting the two traps.

We aim to present the theoretical framework for evaluation of the interaction frequency of two electrons trapped in two separate planar Penning traps. The model we have used for evaluation of the frequency was first introduced in [1]. In our model depicted in Fig(1) we consider two 2-D planar Penning traps connected by a wire which may be dissipative or non-dissipative in nature.

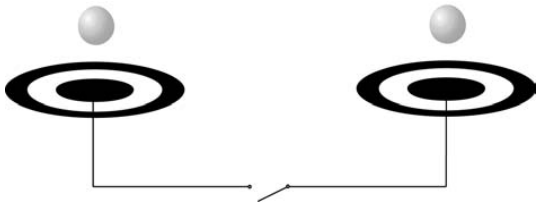

Figure 1. Schematic showing inductive coupling of two electrons

Each trap consists of 4 concentric electrodes, with 3 gaps, where the trap geometry considered is from a recent work [3]. The two traps are assumed to be completely symmetric. The interaction frequency of the two electrons is the rate at which the two electrons exchange their motional energy, similar to two coupled harmonic oscillators. The expression for the frequency is given as:

$$\omega_{int} = \frac{q^2C^2}{8\pi^2\epsilon_o^2R^4m\omega_z}\cdot\frac{1}{2C+C_w}\left(1-\frac{z_o}{\sqrt{R^2+z_o^2}}\right)^2$$

where

q = Charge on electrons
C = Capacitance of the central electrode of the trap
R = Radius of central electrode of the trap
m = Mass of electron
ω_z = Oscillation frequency of the electron
C_w = Capacitance of the connecting wire
z_o = Equilibrium position of the electron above the central electrode.

The capacitance for the planar Penning trap is evaluated using simulations done in COMSOL software and is found for the configuration with R $\approx$ 0.5mm, to be equal to 0.24 pF. We have also evaluated the capacitance of the trap corresponding to the geometry provided in [3], thecapacitance for this geometry comes out to be $\approx$ 2.73 fF. Here is the table giving the approximate interaction frequencies corresponding to these cases, when the capacitance of the wire is assumed to be negligible:

Table 1. Interaction frequency for various values of electron oscillation frequencies

Radius of central electrode R	Electron oscillation frequency ω_z	Interaction frequency ω_{int}
0.5mm	100MHz	32KHz
10μm	4GHz	5.05MHz

References

[1] Stahl S. *at.el.* 2005 *Eur. Phys. J. D* **32** 139-146
[2] Jorge R. *at.el.* 2008 *New J. Phys.* **10** 083021
[3] Kedar Mal *at.el.* 2026 arXiv:2608.17984v1
[4] Bohman M. *at.el.* 2018 Journal of Modern Optics **65** 568-576

†E-mail: geet29@gmail.com

Photostability of isolated nucleotides under ultraviolet radiation

Abheek Roy[1†] and S Sunil Kumar[1]

[1]Indian Institute of Science Education and Research (IISER) Tirupati, 517619, India

The stability of biological molecules under ultraviolet (UV) irradiation has been one of the most extensively investigated problems in molecular photochemistry over the past several decades [1–3]. Among these biomolecules, nucleotides are of particular importance as they constitute the fundamental chemical building blocks of nucleic acids, which encode genetic information and participate in virtually every cellular process essential for life [2]. Photoexcited nucleotide anions, including deoxyadenosine monophosphate ($[dAMP–H]^-$) and adenosine monophosphate ($[AMP–H]^-$), predominantly relax via non-radiative pathways leading to fragmentation. In these systems, photon absorption is followed by internal conversion to the ground state, after which the redistribution of internal energy across vibrational modes leads to statistical fragmentation [4].

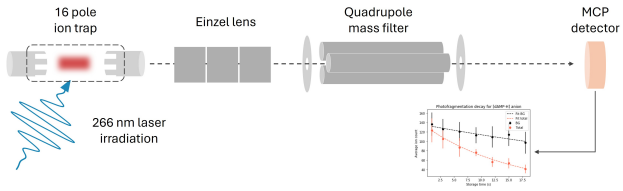

Figure 2: Schematic of the experimental setup for measuring absolute photofragmentation cross sections of trapped nucleotide anions using 266 nm laser irradiation.

In this work, we investigate the UV photofragmentation of isolated $[dAMP–H]^-$ and $[AMP–H]^-$ anions at 266 nm. Absolute photofragmentation cross sections are experimentally determined for both nucleotide systems, providing a quantitative measure of their susceptibility to UV-induced dissociation. Interestingly, despite the structural difference between the deoxyribose and ribose moieties, the measured absolute fragmentation cross sections of $[dAMP–H]^-$ and $[AMP–H]^-$ are found to be comparable within experimental uncertainty, suggesting similar overall photostability under 266 nm irradiation.

To elucidate the molecular origin of the observed fragmentation, time-dependent density functional theory (TD-DFT) calculations are employed to characterize the electronic excitation spectra and relevant excited-state transitions of both anions. Potential fragmentation pathways are subsequently investigated through electronic-structure calculations, with transition-state structures and corresponding barrier heights determined for the different dissociation channels. The calculated barriers are combined with statistical unimolecular rate theory using RRKM analysis. For $[dAMP–H]^-$, an inverse RRKM approach is employed to estimate the effective dissociation barrier by constraining the calculated rates using fragmentation timescales reported in the literature. For $[AMP–H]^-$, the calculated transition-state barrier is used within the RRKM framework to estimate the unimolecular fragmentation rate at the 266 nm excitation energy.

The combined experimental and theoretical analysis links photofragmentation cross sections with molecular structure, dissociation barriers, and fragmentation dynamics, providing insight into the UV response of $[dAMP–H]^-$ and $[AMP–H]^-$ anions

References

[1] Hussain R. *et al.* 2018 *Molecules* **23** 1906
[2] Rastogi R. P. *et al.* 2010 *J. Nucleic Acids* **2010** 592980
[3] Serrano-Andrés L. *et al.* 2008 *Chall. Adv. Comput. Chem. Phys.* **5** 435–472
[4] Sunil Kumar S. *et al.* 2011 *J. Phys. Chem. A* **115** 3483–3490

†E-mail: abheek.roy@students.iisertirupati.ac.in

Dynamical States of Driven Few-Ion Crystals

Vaibhav Mahendrakar[1†], **A. Ayyadevara**[1], **A.Baganali**[1], **J.Hazra**[1], **S. A. Rangwala**[1]

[1]Raman Research Institute, C. V. Raman Avenue, Sadashivanagar, Bengaluru 560080, India

We simulate the dynamics of few-ion crystals driven away from equilibrium through controlled, asymmetric dissipation [1]. They indicate a transition from a minimum energy configuration to persistent collective motion. We characterize the resulting states and their dependence on the competing dissipative processes and the underlying trap confinement. Our results demonstrate how controlled driving can generate sustained non-equilibrium states [2] in a few-body Coulomb system. The latest simulation and the experimental results will be presented in the poster.

References

[1] C. F. P. Avalos, G. A. Prataviera and M. C. de Oliveira. 2025 *arXiv* **2512.18481** 23 Dec 2025

[2] Tony E. Lee and M. C. Cross. 2011 *Phys. Rev. Lett.***106** 143001

[†]E-mail: mahendrakar@rrimail.rri.res.in

Kinetic Monte Carlo Modelling of Recurrent Fluorescence in PAH Cations for the Delhi Penning Trap

S R Kale[1,†], S Bernitt[2], U Kadhane[1], W Quint[2], C P Safvan[3], C P Veena[3], M Vogel[2] and S Kumar[3]

[1]Indian Institute of Space Science and Technology (IIST), Valiamala, Kerala 695547, India
[2]GSI Helmholtzzentrum für Schwerionenforschung GmbH, Planckstraße 1, 64291 Darmstadt, Germany
[3]Inter-University Accelerator Centre (IUAC), Aruna Asaf Ali Marg, New Delhi 110067, India

Synopsis Recurrent fluorescence (RF) can stabilise highly excited polycyclic aromatic hydrocarbon (PAH) cations against fragmentation. We present a kinetic Monte Carlo (KMC) model of RF, infrared (IR) cooling and dissociation, benchmark it against tetracene storage-ring data, and predict that RF from PAH cations in the Delhi Penning Trap (DPT) is observable under detuned MeV electron excitation.

Polycyclic aromatic hydrocarbons (PAHs) are widespread in interstellar environments, where they are identified through their infrared (IR) emission bands. UV photons and cosmic rays, including relativistic electrons, can deposit enough energy in PAHs to raise them above their dissociation thresholds. Although IR emission provides a cooling pathway, the dissociation rate increases rapidly with internal energy, raising the question of how highly excited PAHs survive. Recurrent fluorescence (RF), in which optical photons are emitted from electronically excited states thermally repopulated through inverse internal conversion, provides an additional cooling mechanism. By removing energy in eV-scale quanta, RF can stabilise PAH cations above their dissociation thresholds, as shown in storage rings [1].

Model: To describe this competition, we developed a kinetic Monte Carlo (KMC) framework with three parts. An energy-distribution module provides the initial internal-energy distribution $P(E_0)$. A rate module provides $k_{\mathrm{RF}}(E)$, $k_{\mathrm{IR}}(E)$ and $k_{\mathrm{diss}}(E)$. A propagator follows each ion using the Gillespie algorithm: waiting times are sampled as $\Delta t = -\ln U/k_{\mathrm{tot}}(E)$, with $k_{\mathrm{tot}} = k_{\mathrm{RF}} + k_{\mathrm{IR}} + k_{\mathrm{diss}}$ and U a uniform random number, and each event is chosen with probability k_i/k_{tot}. RF and IR events reduce E by the corresponding photon energy, whereas dissociation terminates the trajectory. Averaging over many trajectories gives survival probabilities and RF photon statistics.

Benchmark: The framework was tested with the tetracene ($C_{18}H_{12}^{+}$) rates of Bernard *et al.* [1] (measured RF, theoretical IR and literature dissociation rates). For $E_0 = 7.0$–9.4 eV, the simulated dissociation fractions follow the branching ratio $k_{\mathrm{diss}}/k_{\mathrm{tot}}$ (Fig. 1) and exceed it slightly at the highest energies, where ions can dissociate after emitting IR photons.

DPT predictions: The Delhi Penning Trap (DPT) [1, 2] combines a 1.1 T Penning trap with radial optical access and the 1–8 MeV electron beam of the Delhi Light Source (DLS) at IUAC [2]. With full beam–ion overlap, fragmentation dominates. When the beam is detuned, the ions are excited by its electromagnetic field and recurrent fluorescence competes with dissociation; 83 % of the ions survive and each emits on average 0.2 RF photons per 10 ms, corresponding to $\sim 2 \times 10^5$ photons s^{-1} for 10^4 stored ions.

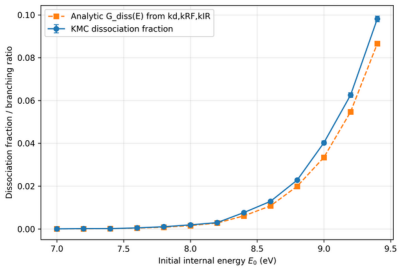

Figure 1. KMC and analytic dissociation fractions for tetracene.

References

[1] Bernard J *et al.* 2023 *Phys. Chem. Chem. Phys.* **25** 10726
[2] Kumar S *et al.* 2026 *Mon. Not. R. Astron. Soc.* **548** stag684
[3] Kumar S *et al.* 2025 *J. Instrum.* **20** C05016
[4] Ghosh S *et al.* 2017 *Nucl. Instrum. Meth. B* **402** 358

[†]E-mail: shravan.sc23b192@ug.iist.ac.in

Non-Invasive Room-Temperature Detection of a Single Trapped Electron in VECC Penning Trap

Arindam Kr. Sikdar[1,2†], Joydip Nandi[1], B. Chakraborty[3] , A. Biswas[3] , A. Ray[1], K.T. Satyajith[4], and Parnika Das[1,2]

[1]Variable Energy Cyclotron Centre, 1/AF, Bidhannagar, Kolkata, INDIA
[2]Homi Bhabha National Institute, Anushaktinagar, Mumbai, Maharashtra, INDIA
[3]Jadavpur University, Raja Subodh Chandra Mallick Road, Jadavpur, Kolkata, INDIA
[4]Delta Q, IMJ Institute of Research, Moodlakatte, Karnataka, INDIA

Synopsis We demonstrate a simple room-temperature method for detecting a single trapped electron without cryogenic electronics or image-current readout. The confined electron ionizes residual gas molecules, producing low-energy ions that are guided to a Microchannel Plate (MCP) and counted individually. These ion bursts provide a sensitive signature of single-electron confinement. Fano-factor analysis and Pearson correlation distinguish the single-electron signal from background and multi-electron conditions, establishing a robust, non-invasive approach to single-electron detection at room temperature.

A non-invasive technique is devised for detecting a single electron confined in a room-temperature Penning trap through ionization of residual background gas. Primary 145 eV electrons are generated using a custom fabricated Carbon-Nanotube-based Electron Gun (CNEG) and loaded by pulsing the upper endcap facing the source, as shown in Figure 1. The electron transit time from the upper to lower endcap, including reflection from the −500 V lower endcap, is around 2–4 ns. Electrons arriving within this window are captured when the upper endcap is switched from 0 to −500 V.

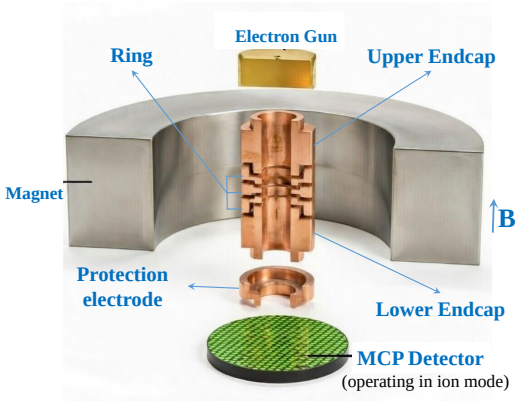

Figure 1. VECC Penning Trap assembly

The confined electron ionizes residual gas molecules, producing low-energy ions that are extracted, guided to a MCP by a +300 V ring-electrode potential and detected individually. Background measurements of ion hit pattern over 500 cycles of 100 milli-seconds each gave a Fano factor near unity and a Pearson coefficient of 0.14, indicating predominantly random ionization [1]. When CNEG was biased to −145 V, corresponding to 0.5–1 electron per micro-second, the Fano factor increased to 1.42 and the Pearson coefficient to 0.24, indicating a common electron-induced ion source. Higher CNEG voltages produced more than two stored electrons, yielding a Fano factor of 1.7 and a Pearson coefficient of 0.01, respectively, while lower voltages reproduced background statistics. These results demonstrate single-electron confinement through statistical ion detection and provide a practical room-temperature alternative to conventional cryogenic image-current detection [2, 3]. Beyond direct detection, this technique provides a potential pathway toward developing a high-fidelity single-electron source, which could enable sensitive charge and force measurements, precision sensing, and emerging quantum-information technologies requiring controlled single-electron generation and manipulation.

References

[1] Benjamin Crockett *et al.* 2022 *Laser Photonics Rev.* **16** 2100635
[2] Lowell S. Brown and Gerald Gabrielse 1986 *Rev. Mod. Phys.*, **58** 233
[3] D. M. Asner *et al.* 2015 *Phys. Rev. Lett.* **114** 162501

†E-mail: aksikdar@vecc.gov.in

Identification and consolidation of decay hierarchy of statistical fragmentation network in aromatic molecules and their fragments

Binduja Panja[1†], **Umesh R Kadhane**[1†]

[1]Atomic and Molecular Physics Laboratory, Indian Institute of Space Science and Technology, Thiruvananthapuram, 695547, India

Synopsis The internal-energy-dependent fragmentation of a systematically connected series of aromatic molecules and their ionic fragments is investigated using complementary ionization and dissociation methods. Energy-correlated time-of-flight measurements establish precursor–product relationships and resolve fragmentation pathways as a function of internal energy, including the subsequent dissociation of reactive ionic fragments that are difficult to study as standalone species. Moreover, consolidation is provided with the help of low electron impact and collision induced dissociation measurements and DFT calculations.

The identification of individual polycyclic aromatic hydrocarbons (PAHs) in the interstellar medium (ISM) remains challenging, particularly because many symmetric PAHs possess no permanent electric dipole moment and are therefore not readily accessible through conventional rotational spectroscopy. Laboratory studies of their ionization and fragmentation under different energetic conditions are consequently important for understanding the chemical evolution of aromatic species in space. A systematically connected series of aromatic molecules is investigated, from benzene and toluene to naphthalene, 1- and 2-methylnaphthalene, ethylnaphthalene, indene, and indole. This molecular progression enables the effects of ring fusion, alkyl substitution, and heteroatom incorporation on internal-energy-dependent dissociation to be examined. The molecules are subjected to complementary energetic conditions using electron-impact ionization (EI), 266 nm multiphoton ionization (MPI), and, for selected species, proton-impact ionization at the LEIBF facility, IUAC. EI measurements are performed using a commercial quadrupole mass analyzer, while MPI measurements employ a high-resolution energy-correlated time-of-flight mass spectrometer equipped with an electrostatic parallel-plate analyzer (PPA) [1].

The PPA separates ions according to their kinetic energies, allowing prompt and delayed fragmentation products to be distinguished. Systematic variation of the PPA voltage establishes precursor–product relationships and resolves internal-energy-dependent dissociation pathways. Although conceptually related to tandem mass spectrometry (MS/MS), the energy-correlated approach provides far superior selectivity in the identification of decay hierarchy. The method is applied not only to conventional molecular ions but also to the ionic fragments generated from them. Coupling the ToF platform to a collision cell further enables collision-induced dissociation (CID) of selected ionic fragments, allowing their subsequent fragmentation pathways to be investigated, including whether they preferentially undergo H or H_2 loss or eliminate larger neutral hydrocarbon fragments.

Hence, a key aspect of this work is the investigation of ionic fragments that may be chemically reactive and difficult to study as standalone species. By generating these ions from well-characterized molecular precursors and combining experimental measurements with DFT calculations, their subsequent dissociation can be examined to understand how molecular structure and internal energy govern the competing fragmentation pathways.

References

[1] Vinitha M V, Kala A, Kumar S and Kadhane U R 2019 *Rev. Sci. Instrum.* **90** 103301.

[†]E-mail: bindujapanja24@gmail.com
[†]E-mail: rkumesh@gmail.com

Part III

Contributed Abstracts

Design, Development, and Characterization of a Dual Linear Paul Trap

J Hazra [1†], V Mahendrakar[1], A Baganali[1], A Ayyadevara[1], M Ibrahim[1], A Bhowmick[2], S.A. Rangwala[1]

[1]Raman Research Institute, C. V. Raman Avenue, Sadashivanagar, Bengaluru 560080, India

[2]Manipal Institute of Technology, Yelahanka, Bengaluru 560064, India

Synopsis We report the implementation and initial characterization of a dual-site linear Paul trap for confining Ca ions.

Here, we report the design, assembly, and initial characterization of a dual linear Paul trap, for confining Ca ions. The system is assembled within a vacuum chamber, with three atomic calcium ovens [1] integrated to allow simultaneous loading in the trap sites. A high-voltage radio-frequency drive is delivered via a custom-developed helical resonator [2] [3] to operate the trap. An imaging system with 15X-20X magnification has been designed [2] and implemented to detect ion fluorescence in both traps using a single-photon counting head. Resonant tickle excitation is subsequently employed to determine the radial and axial secular frequencies of the trapped ^{40}Ca ions. This system is being developed towards ion transport [4], scalability [5], coherent control of qubit transitions [6], and studies of fundamental physics. This is an ongoing experiment; recent developments and progress will be presented in the poster.

References

[1] Prakash A *et al.* 2024 *Review of Scientific Instruments* **95** 033202
[2] Prakash A *et al.* 2026 *AIP Advances* **16** 075202
[3] Ballance C 2017 *High-Fidelity Quantum Logic in Ca+* Book ?
[4] Pedregosa-Gutierrez J *et al.* 2015 *International Journal of Mass Spectrometry* **381–382** 33
[5] Ravi K *et al.* 2010 *Phys. Rev. A* **81** 031401(R)
[6] Häffner H *et al.* 2008 *Physics Reports* **469** 155–203

[†]E-mail: jhilik@rrimail.rri.res.in

Formation of Nitrogen-Bearing PAHs: An Efficient UV-Induced Pathway in the Interstellar Medium

P. Thakkar[1], S. S. Payra[1], Y. Lenka[1], S. K. Pandit[2], S. Nath[2], K. R. Nandipati[2] and G. Aravind[1†]

[1]Department of Physics, Indian Institute of Technology Madras, Chennai, 600036, India

[2]Department of Chemistry, Indian Institute of Technology Madras, Chennai, 600036, India

Synopsis Using a 22-pole rf ion trap, we demonstrate that 266 nm UV photoionization of pyridine drives coupled top-down fragmentation and bottom-up molecular growth. The resulting reactive ionic fragments facilitate the formation of polycyclic aromatic nitrogen heterocycles (PANHs), offering key mechanistic insights into chemical evolution within photodissociation regions, circumstellar envelopes, and Titan's atmosphere.

The photochemical processing of polycyclic aromatic hydrocarbons (PAHs) and their nitrogen-bearing analogs (PANHs) in the interstellar medium and in (exo)planetary atmospheres is often considered as a predominantly destructive process. Here we show that UV-driven fragmentation of pyridine, the simplest Nitrogen heterocycle, simultaneously generates reactive intermediates capable of efficient bottom-up molecular growth toward larger, more complex PANHs. Using a 22-pole radiofrequency ion trap, we investigate how reactive photofragments produced by dissociative ionization of pyridine (C_5H_5N, m/z 79) at 266 nm subsequently undergo ion–neutral reactions at room temperature. The dominant fragmentation channel, loss of HCN/HNC, produces $C_4H_4^{\bullet+}$ (m/z 52), a mixture of the cyclic methylenecyclopropene radical cation ($MCP^{\bullet+}$) and the open-chain vinylacetylene radical cation ($VA^{\bullet+}$) [1].

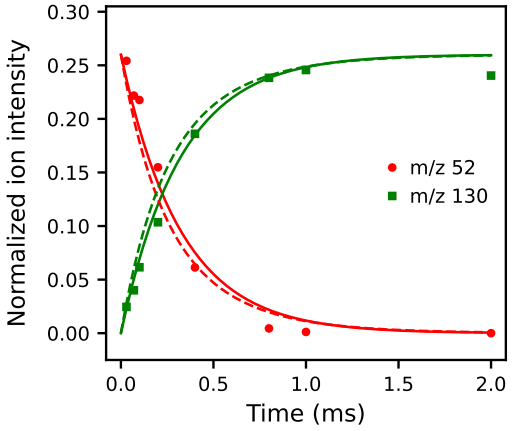

Figure 1. Time evolution of $C_4H_4^+$ (m/z 52) and the reaction product $C_9H_8N^+$ (m/z 130) in the presence of pyridine at a number density of $(3.0 \pm 0.9) \times 10^{12}$ molecules cm^{-3}. Markers represent the experimental data. The solid and dotted lines correspond to the reduced ODE and bi-exponential ODE model fits, respectively. Ion intensities are normalized to the total ion counts in each trapping cycle.

References

[1] Rap *et al.* 2023 *Faraday Discussions* **245** 221244

[2] D S N Parker *et al.* 2019 *Proceedings of the National Academy of Sciences* **109** 5358

†E-mail: garavind@iitm.ac.in

Probing a New Formation Pathway for N-bearing PAHs in the Interstellar Medium Using a 22-Pole Ion Trap

Y Lenka[1], S S Payra[1], P Thakkar[1], K R Nandipati[2] and G Aravind[1†]

[1]Department of Physics, Indian Institute of Technology Madras, Chennai, 600036, India

[2]Department of Chemistry, Indian Institute of Technology Madras, Chennai, 600036, India

Synopsis We investigate the reaction of pyrimidine cations with acetylene using a modified 22-pole radio-frequency ion trap. Time-resolved mass spectrometry reveals sequential acetylene addition. The measured kinetics provide rate coefficients for radiative association and subsequent bimolecular reactions, constraining nitrogen-bearing molecular growth in astrochemical environments.

Ion-molecule reactions are considered important pathways to facilitate molecular growth in interstellar and planetary environments. Where low densities can favor reaction mechanisms that differ from those observed under conventional laboratory conditions. Here, we investigate the reaction between pyrimidine cations ($C_4H_4N_2^+$) and acetylene (C_2H_2) using a modified 22-pole radio-frequency ion trap.

Pyrimidine is ionized by electron impact, mass-selected using a quadrupole mass spectrometer, and injected into the 22-pole ion trap, where Helium buffer gas is used for collisional cooling. C_2H_2 is then subsequently introduced into the trap at controlled number densities, and the trapped ions are monitored as a function of storage time using a second quadrupole mass spectrometer. This time resolved approach allows the kinetics of sequential ion–molecule reactions to be followed under reduced-density conditions.

The reaction initially produces an m/z 106 species through bimolecular association of acetylene with pyrimidine ions. At higher acetylene densities and longer storage times, the m/z 106 intermediate undergoes hydrogen abstraction acetylene addition reaction, producing a product at m/z 131. Kinetic modelling of the measured ion populations gives a radiative association rate coefficient of $k_{\mathrm{RA}} = (1.3 \pm 0.3) \times 10^{-10}\ \mathrm{cm}^3, \mathrm{s}^{-1}$ for the initial reaction. The subsequent reactions are characterized by $k_1 = (3.4 \pm 1.1) \times 10^{-13}\ \mathrm{cm}^3, \mathrm{s}^{-1}$ and $k_2 = (2.2 \pm 0.9) \times 10^{-12}\ \mathrm{cm}^3, \mathrm{s}^{-1}$. [1]

Electronic-structure calculations support a sequential reaction mechanism leading to a stable bicyclic nitrogen-bearing cation through an overall exothermic pathway. These results demonstrate the capability of the 22-pole ion-trap technique for studying sequential molecular growth reactions under conditions relevant to astrophysical environment.

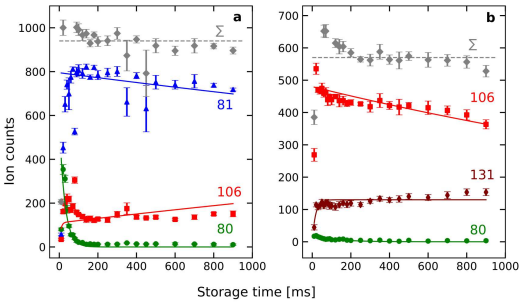

Figure 1. Time-resolved ion counts for pyrimidine and protonated pyrimidine reacting with C_2H_2 at 295 K under (a) low and (b) high acetylene number densities. Solid lines show ODE-model fits; gray dots denote the total ion counts.[1]

References

[1] Payra S S *et al.* 2026 *The Astrophysical Journal* **ApJ 1008 212**

†E-mail: garavind@iitm.ac.in

A 22-pole ion trap setup for astrophysically relevant reaction kinetic studies

Siddhartha S. Payra[†], **Pratikkumar Thakkar, Yash Lenka, G. Aravind**[†]

Indian Institute of Technology Madras, Chennai, 600036, India

Synopsis Astronomical detection has identified the presence of complex molecules in extraterrestrial environments, yet their formation and evolution are poorly understood. Ion–molecule reactions are believed to play an important role in shaping their observed abundances. We have developed a 22-pole radio-frequency ion trap to investigate the kinetics of such reactions under controlled conditions. We present a systematic characterization of the setup and improvements to enable reliable determination of neutral-gas density and reproducible reaction rate coefficients.

Over the past several decades, more than 300 molecules have been detected in the interstellar medium. The formation mechanisms of these astromolecules remain an open question. The discrepancies between their predicted and observed abundances point to unknown mechanisms such as ion-molecule reactions that govern their evolution in astrophysical environments [1]. To study the kinetics of such cosmically relevant ion-molecule reactions under controlled laboratory conditions, we built a 22-pole radio frequency ion trap setup.

The experimental setup consists of an ion source, two quadrupole mass spectrometers, one 22-pole ion trap, and one channel electron multiplier detector, in the arrangement shown in Fig.1. A detailed description of all parts can be found in [2]. This apparatus can be used to measure reactions between cations and neutral molecules as a function of time, neutral gas density, and temperature. In addition, a laser beam horizontal to the spectrometer axis can be coupled with the ion trap to study the photon-induced ion-neutral reactions.

Here we discuss the results of all tests that have been done to investigate the influence of different experimental parameters and modifications to improve the ion trap setup. A major modification was carried out in order to measure the neutral density, which is essential for measuring reaction rate coefficients. For this, a capacitive gauge was directly connected to the trap volume. Furthermore, an experimental procedure will be described in order to get reliable and reproducible results for ion-molecule reaction rate coefficients. These developments provide a robust platform for quantitative studies of ion–molecule kinetics relevant to astrophysical environments.

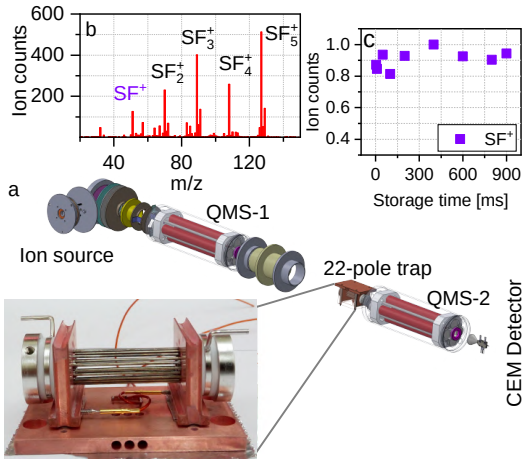

Figure 1. Schematic drawing of the modified 22-pole radio frequency ion trap setup (a). The ions are produced by a discharge or electron impact ion source and analyzed using first quadrupole mass spectrometer (QMS-1). A sample mass spectrum obtained upon discharge of SF_6 gas was shown here (b). Mass-selected SF^+ was injected into the ion trap and trapped for $\sim 1s$ (c). A second quadrupole mass spectrometer (QMS-2) was used for analysing the contents of the trap and detected using a channel electron multiplier (CEM) detector.

References

[1] Siddhartha S P *et al.* 2026 *APJ* **1008** 212
[2] Nihar R B *et al.* 2024 *RSI* **95** 013201

[†]E-mail: ph23d029@smail.iitm.ac.in
[†]E-mail: garavind@iitm.ac.in

Delhi Penning Trap Setup For Experimental Study of Electron-Impact Ionization Cross-Section in Relativistic regime

Avnish Ola[1†], Tufail Khan[3], Veena C.P.[2], Kedar Mal[2], Sugam Kumar[2], C.P. Safvan[2], W. Quint[4], M. Vogel[4], Punita Verma[5]

[1]Department of Physics and Astrophysics, University of Delhi, New Delhi, 110007, India
[2]Inter University Accelerator Center, Aruna Asaf Ali Marg, New Delhi, 110067, India
[3]Jamia Millia Islamia University, Jamia Nagar, New delhi, 110025, India
[4]GSI Helmholtzzentrum Fur Schwerionenforschung, Darmstadt, 64291, Germany
[5]Department of Physics, Kalindi College, University of Delhi, New Delhi, 110008, India

The Delhi Penning Trap (DPT)[1] has been developed as a dedicated facility for controlled studies of electron–ion interactions, with the long-term objective of investigating EII cross-section at relativistic electron energies. The cryogenic cylindrical Penning trap enables confinement and manipulation of ions under ultra-high-vacuum conditions, providing a low-background environment for precision measurements.

The DPT incorporates both destructive and non-destructive detection approaches for characterizing trapped ions and ionisation products. Non-destructive detection allows ions to be monitored without removing them from the trap, whereas destructive detection involves extracting the ions for subsequent identification based on their mass-to-charge ratio. During the initial commissioning of the facility, Electron-Ion interaction were performed using a 1 keV electron gun with helium, nitrogen, and argon as test gases. The ionisation products were extracted from the trap and analysed using a time-of-flight (TOF) technique, providing mass-to-charge-dependent identification of the produced ions.

The obtained TOF measurements are used to validate the ion trapping, electron-beam interaction, ion extraction, and detection systems. The facility is ultimately intended to measure EII cross-section into the 1–8 MeV energy range generated using FEL(Free Electron Laser)[2] based electron source, enabling experimental investigation of relative ionisation cross-section in the relativistic energy regime. We are going to measure relative cross-section not absolute because to measure it we need density of target gas and length of interaction region which is impossible to calculate in our experiment setup.

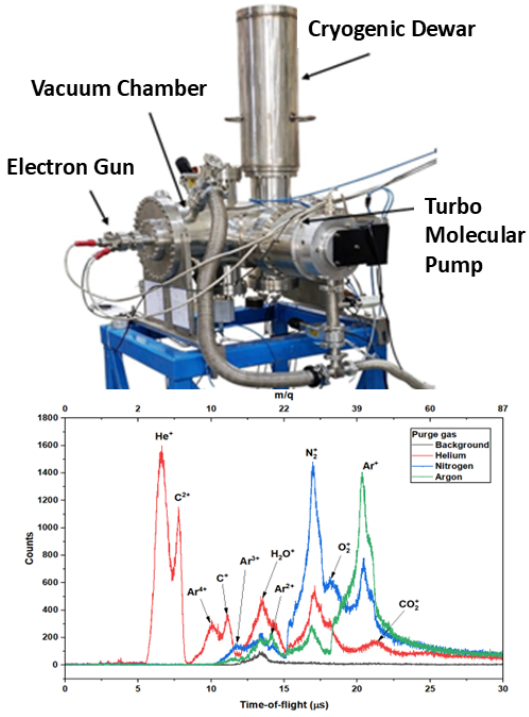

Figure 1. Delhi Penning Trap setup and graph of TOF of He,N_2 and Ar gas.

References

[1] Kumar S *et al.* 2025 *J. Instrum.* **20** C05016
[2] Ghosh S *et al.* 2017 *Nucl. Instrum. Methods Phys. Res. B* **402** 358–363
[3] Scholz W*et al.* 1972 *phys. Rev. Lett.* **29** 761
[4] Santos J P M D, Parente F A D F C *et al.* 2012 *Int. J. Mass Spectrom.* **313** 1–7

†E-mail: avnish.phd2025@physics.du.ac.in

Design and Optimization of a Multilayer Axial Resonator for Ar^+ Detection in the Delhi Penning Trap (DPT)

Veena C P[1†], Kedar Mal[1], Avnish Ola [2], Sanjeev Kumar Thakur [1], Sugam Kumar[1], C.P. Safvan[1], W. Quint[3] and M. Vogel[3]

[1]Inter University Accelerator Center, Aruna Asaf Ali Marg, New Delhi, 110067, India
[2]Department of Physics and Astrophysics, University of Delhi, New Delhi, 110007, India
[3]GSI Helmholtzzentrum Fur Schwerionenforschung, Darmstadt, 64291, Germany

Synopsis Resonators are widely used for the non-destructive detection of trapped ions in Penning traps through resonant image-current detection. The performance of such resonators depends strongly on their inductance, parasitic capacitance, and self-resonance frequency, which are influenced by the winding geometry and number of winding layers. This work investigates the design and characterization of multilayer helical resonators, with emphasis on understanding the dependence of these parameters on the number of winding layers.A theoretical model was validated against experimental measurements and used to optimize the resonator design.

Non-destructive detection of trapped ions using resonant image-current detection is an important technique for characterizing the ions in Penning traps. In this work, an axial resonator has been designed for the detection of Ar^+ ions in the Delhi Penning Trap (DPT). For the trap parameters $B_0 = 1.0$ T, $C_2 = 0.62$, and $d = 3.67$ mm, an operating trap voltage of approximately 17.8 V corresponds to an axial frequency of about 223 kHz for Ar^+ ions [1].

Initially a multilayer helical resonator was fabricated and characterized using frequency-response measurements with different external capacitances. The measured inductance was 27.3 mH, close to the calculated value, whereas the measured self-capacitance was 57.3 pF, which was higher than the initial estimate of 25 pF. This resulted in a measured self-resonance frequency of approximately 128 kHz.

To understand the observed discrepancy, a separate multilayer test resonator was fabricated and characterized for different numbers of winding layers. The measured inductance, parasitic capacitance, and self-resonance frequency were compared with theoretical models for multilayer windings [2]. The hexagonal-winding model showed good agreement with the experimental results, with average deviations of approximately 7% in inductance, 8% in capacitance, and 3% in resonance frequency. The validated model was subsequently applied to redesign the axial resonator.

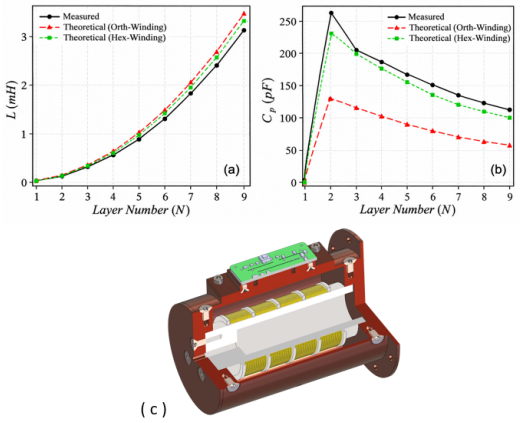

Figure 1. Comparison of theoretical and experimental (a) self-inductance and (b) parasitic capacitance as a function of winding layers, and (c) SolidWorks model of the resonator assembly.

Hence a three-layer resonator was designed with a calculated self-inductance of approximately 2.95 mH and self-capacitance of 116.95 pF, the predicted resonance frequency is approximately 218 kHz, close to the required 223 kHz axial frequency of Ar^+ ions.

References

[1] Kumar S *et al.* 2025 *J. Instrum.* **20** C05016
[2] Wan L *et al.* 2023 *IEEE Access* **11** 134460–134472

†E-mail: cpveenakkkt@gmail.com

From electrode asymmetry to octupole anharmonicity: quantum motional dynamics of a single ion in a Paul trap

S Jana[1†], A Dey[1], P Mandal[2] and N Deb[1†]

[1]School of Chemical Sciences, Indian Association for the Cultivation of Science, Kolkata 700032, India
[2]Department of Physics, St. Paul's Cathedral Mission College, Kolkata-700009, India

Synopsis Radial diagonal asymmetry in round-rod quadrupole devices generates octupole fields that are absent in the symmetric geometry. Building on our earlier SIMION studies of these fields, we treat the resulting quartic anharmonicity quantum mechanically for a single ion in an RF Paul trap. The octupole term opens $\Delta n = \pm 4$ channels and adds occupation-dependent phase shifts: the phonon-number variance rises by ∼18% against ∼6% for the mean, while RF-generated quadrature squeezing survives but is weakened and reoriented.

In symmetric round-rod traps only dodecapole and icosapole harmonics accompany the quadrupole field, but any radial asymmetry breaks the fourfold symmetry. Using SIMION simulations, we showed that changing the radius of a single rod [1], or displacing or resizing a diagonal rod pair [2], generates octupole (A_4) and hexadecapole (A_8) components that grow with the asymmetry parameter γ (Fig. 1a). Classically, they shift the stability apex, broaden the transmission contour and degrade the resolution in step with $|A_4| + |A_6|$ [1, 2]. The octupole is thus the leading, practically unavoidable, anharmonic correction to the trapping field.

Here we ask what it does to the *quantized* ion motion. We retain the full RF time dependence, $V = (m\Omega^2/8)(a + 2q\cos\Omega t)(x^2 + \lambda x^4)$ with $\lambda = A_4/r_0^2$, and work in the Fock basis of a reference oscillator, $\omega_0 = \sqrt{a}\,\Omega/2$. The quadratic RF term couples $\Delta n = \pm 2$ and squeezes; the quartic term adds $\Delta n = \pm 4$ couplings and a Kerr-like diagonal shift $\propto 6n^2 + 6n + 3$. Parity conservation confines an initial vacuum to the even ladder. The Schrödinger equation ($N = 80$, converged to $N = 120$) is integrated over 1000 RF cycles at $a = 0.1$, $q = 0.5$ for $\lambda = A_4\ell_\Omega^2/r_0^2 \le 5 \times 10^{-4}$, $\ell_\Omega = \sqrt{\hbar/m\Omega}$.

The octupole builds a weak, converged population tail up to $n \approx 80$. Since $\langle n^2\rangle$ weights it by n^2, the cycle-averaged variance rises from 1.59 to 1.88 while $\langle n\rangle$ moves only from 0.485 to 0.515; the Mandel parameter grows from 2.27, already large from RF pair creation, to 2.65. Quadrature squeezing is robust: $S_{\min} < 0$ at every RF phase of the 1000th cycle, with $(\Delta X_s)^2 = 0.102$ versus 0.086 without the octupole (vacuum 0.5). It is, however, reduced and reoriented (Fig. 1b), as n-dependent phases dephase $\langle \hat{a}^2\rangle = \sum_n \sqrt{(n+1)(n+2)}\, c_n^* c_{n+2}$.

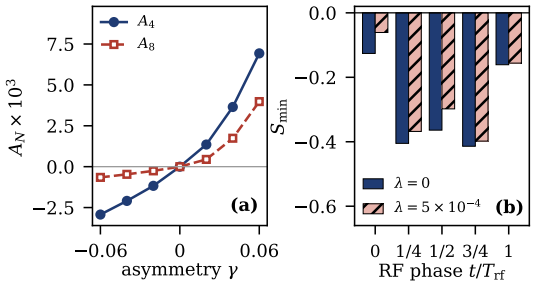

Figure 1. (a) Octupole (A_4) and hexadecapole (A_8) coefficients versus single-rod asymmetry γ ($\eta = 1.14$) [1]. (b) Minimum squeezing parameter $S_{\min}$ at five phases of the 1000th RF cycle ($a = 0.1$, $q = 0.5$).

Number and quadrature fluctuations thus respond oppositely to the same perturbation (Fock-space spreading versus phase-space shearing), linking the multipole analysis of imperfect traps [1, 2] to nonclassical motional-state control [3].

References

[1] Jana S *et al.* 2025 *Int. J. Mass Spectrom.* **517** 117495
[2] Jana S *et al.* 2025 *J. Am. Soc. Mass Spectrom.* **37** 180-187
[3] Leibfried D *et al.* 2003 *Rev. Mod. Phys.* **75** 281

†E-mail: sukanya03jana@gmail.com
†E-mail: nabanita.deb@iacs.res.in

Quantum Beam-Splitter Cooling and Thermometry in Large Trapped-Ion Crystals

K Rajakumar[1,2†], A Das[1,2], A Pandey[1,2] and A Shankar[1,2†]

[1]Department of Physics, Indian Institute of Technology Madras, Chennai 600036, India

[2]Center for Quantum Information, Communication and Computing, Indian Institute of Technology Madras, Chennai 600036, India

Synopsis We propose quantum beam-splitter cooling (QBSC), a protocol for rapid near-ground state cooling of the center-of-mass mode of a large trapped ion crystal via a red-sideband SWAP with the collective spin followed by a spin reset, and quantum beam-splitter thermometry (QBST), which is near-optimal. This work is available as a preprint on arXiv (arXiv:2606.21357) and is currently under review at Physical Review Applied.

This manuscript is available as a preprint on arXiv [1] and is currently under review at Physical Review Applied.

Laser cooling of trapped ions has enabled the exquisite control of single ions and Coulomb crystals of multiple ions for quantum science experiments. Experiments with long ion strings and two-dimensional trapped ion crystals carried out in the strong sideband coupling regime have observed many-body enhancements in the cooling rate of specific motional modes, suggesting that cooling in this regime cannot be treated as independent contributions from individual ions in the crystal.

We propose and characterize a protocol for rapid near-ground state cooling of the center-of-mass (c.m.) mode of a large trapped ion crystal. When the initial mean thermal occupation of the mode $\bar{n}_i$ is small compared to the number of ions N, a red sideband (RSB) drive implements a beam-splitter type SWAP operation between the mode and the collective spin of the N ions, with the latter effectively serving as a quantum harmonic oscillator. Subsequently, a reset of the spins removes the entropy, leading to near-ground state cooling of the c.m. mode. We term this protocol as quantum beam-splitter cooling (QBSC).

We analyze the impact of several practical imperfections on the final temperature achievable under QBSC, including finite ion number, off-resonant carrier and blue-sideband contributions, and the impact of the sideband drives arising from spectator modes. In addition, we outline practical strategies to eliminate the carrier drive.

Furthermore, we show that measuring the population statistics of the ions at the end of the SWAP operation can enable near-optimal quantum beam-splitter thermometry (QBST), with the classical Fisher information approaching the quantum Fisher information of a thermal state. We discuss the connection of QBSC with continuous sideband cooling and compare QBST with a recently proposed rapid adiabatic passage-based thermometry scheme.

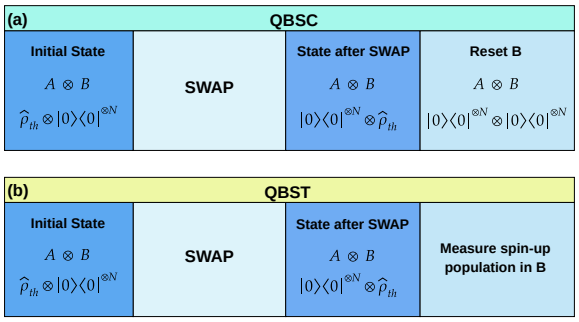

Figure 1. Schematic of the two QBS protocols (reproduced from Fig. 1 of Ref. [1])

Our work constitutes an example of harnessing many-body effects to open new routes to laser cooling and thermometry in large trapped ion crystals.

References

[1] Rajakumar K, Das A, Pandey A and Shankar A 2026 *arXiv:2606.21357* https://arxiv.org/abs/2606.21357

†E-mail: ph25d019@smail.iitm.ac.in
†E-mail: athreya@physics.iitm.ac.in

Towards Paul trapping of single electron bubbles in liquid helium

D Samanta[1†] and A Ghosh[1,2]

[1]Centre for Nano Science and Engineering, Indian Institute of Science, Bengaluru 560012, India
[2]Department of Physics, Indian Institute of Science, Bengaluru 560012, India

Synopsis Single electron bubbles (SEBs) in liquid ^{4}He place an electron spin in a defect-free, nuclear-spin-free host. We present a strongly overdamped surface-electrode Paul trap for SEBs whose trap depth is limited by vortex-ring nucleation, with an operating window at 0.7 K (20–25 V, 0.5 MHz) and a DC-transport and acoustic-cavitation scheme to test confinement.

Solid-state spin qubits are limited by defects, interfaces and magnetic impurities in their host. Electrons floating on liquid helium [1] or solid neon [2] avoid bulk defects but remain bound to a surface. In bulk liquid ^{4}He, an excess electron is repelled by Pauli exclusion and self-traps inside a cavity of radius ≈ 1.9 nm set by zero-point energy, surface tension and pressure. While this single electron bubble (SEB) places the electron spin in a defect-free, nuclear-spin-free liquid, spatially confining the bubble within the bulk liquid remains a central challenge.

To achieve this, we have built a surface-electrode point Paul trap [3] for SEBs (figure 1(a)). A grounded central disk (radius 0.5 mm) concentric with a radio-frequency (RF) ring electrode (outer radius 3.5 mm) forms an on-axis RF electric-field null ≈ 1 mm above the electrode surface.

In liquid ^{4}He at 0.7 K, thermal roton and phonon scattering strongly damps the SEB motion. Its mobility [4] and hydrodynamic mass $m^* \approx 243\, m_{\mathrm{He}}$ give a momentum-relaxation time $\tau \approx 55$ ns, corresponding to $\Omega\tau \approx 0.17$ at $\Omega/2\pi = 0.5$ MHz. In this overdamped regime, the micromotion is supressed and phase-lagged, reducing the pseudopotential depth $\Psi = e^2E^2/[4m^*(\Omega^2 + \tau^{-2})]$ (for RF field amplitude E) by a factor of ≈ 35 compared to vacuum [5]. Here $\Psi = m^* v_1^2/4$ equals the mean micromotion kinetic energy for velocity amplitude v_1. Because an SEB moving faster than $v_c \approx 20\ \mathrm{m\,s^{-1}}$ nucleates and attaches to a quantized vortex ring [6], the trap depth cannot exceed $\Psi_{\max} = m^* v_c^2/4 \approx k_B \times 11.7$ K for any trap geometry or drive frequency. Electrostatic field calculations and driven Langevin simulations place the 0.7 K operating window at $V_{\mathrm{rf}} \approx 20$–$25$ V, giving a well depth of ≈ 7–10 K while keeping $v_1 < v_c$ (figure 1(b)).

We inject SEBs from a ^{63}Ni β-source and detect them by acoustic cavitation [7], using the negative-pressure swing of a focused ultrasound pulse to expand an SEB past its tensile stability limit to an optically detectable size. Because the trap sits above the acoustic focus, a DC-electrode sequence controls the SEB density during loading and then guides trapped bubbles from the RF null into the focus. Comparing cavitation counts with the trap switched on and off provides a direct test of confinement. The experiment is currently underway.

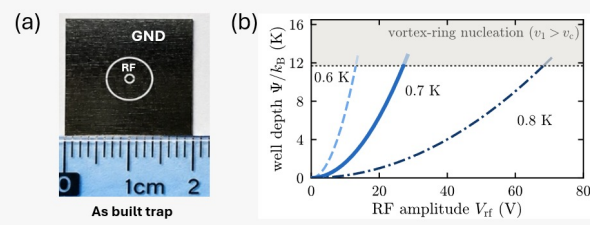

Figure 1. (a) As-built trap. (b) Well depth vs RF amplitude at 0.5 MHz with the vortex-ring nucleation ceiling ($v_1 > v_c$).

References

[1] Platzman P M and Dykman M I 1999 *Science* **284** 1967
[2] Zhou X *et al.* 2022 *Nature* **605** 46
[3] Kim T H, Herskind P F, Kim T, Kim J and Chuang I L 2010 *Phys. Rev.* A **82** 043412
[4] Donnelly R J and Barenghi C F 1998 *J. Phys. Chem. Ref. Data* **27** 1217
[5] Conangla G P, Nwaigwe D, Wehr J and Rica R A 2020 *Phys. Rev.* A **101** 053823
[6] Rayfield G W and Reif F 1964 *Phys. Rev.* **136** A1194
[7] Yadav N, Sen P and Ghosh A 2021 *Sci. Adv.* **7** eabi7128

†E-mail: debnaths@iisc.ac.in

Analysis of an effective adiabaticity parameter to characterize ion temperatures in multipole radiofrequency ion traps

Pragya Nandan[1†] **and S Sunil Kumar**[1]

[1]Indian Institute of Science Education and Research (IISER) Tirupati, 517619, India

Synopsis RF heating keeps buffer-gas-cooled ions in multipole RF traps warmer than the buffer gas, and predicting their temperature needs costly trajectory simulations. We define an effective adiabaticity parameter, η_{eff}, as the adiabaticity parameter averaged over the thermally accessible region of the effective potential. Across ideal and shifted 8-pole, 16-pole and 16-wire traps, it differs more than twofold at 4 K but converges at 300 K.

Radiofrequency (RF) multipole ion traps confine ions radially through the effective potential of an oscillating inhomogeneous electric field, $V^* = q^2E_0^2/4m\Omega^2$, while static endcap electrodes provide axial confinement [1]. Buffer-gas collisions cool the ions, but collisions in the RF field also transfer energy from the field to the ions. This RF heating keeps the ions warmer than the buffer gas, and predicting their temperature normally requires computationally demanding ion-trajectory simulations for every trap geometry and operating condition.

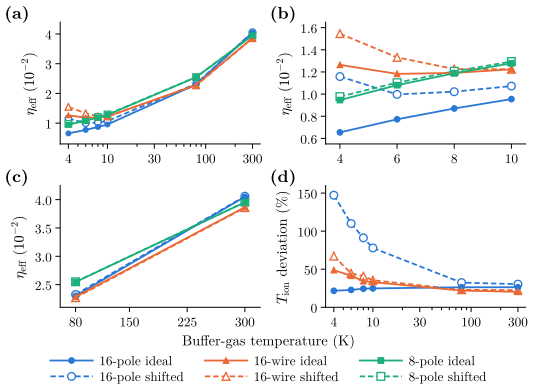

Figure 1. (a) η_{eff} versus temperature; (b, c) low and high ranges. (d) Ion-temperature deviation.

The effective-potential description holds when the RF field changes little over the full distance of the ion's oscillation compared with the field itself. Gerlich expresses this through the adiabaticity parameter $\eta = 2q|\nabla E_0|/m\Omega^2$ and gives $\eta < 0.3$ as the condition for safe operation [1]. This is most critical at the turning point of the ion, where the RF field is strongest and buffer-gas collisions cause RF heating. In real traps, displaced RF electrodes (shifted traps) distort the potential landscape and create minima away from the trap centre [2].

In this work, we introduce an effective adiabaticity parameter, η_{eff}, that accounts for the region occupied by the ions at a given temperature. The total effective potential, the sum of the RF effective potential and the static DC contribution of the endcaps (10 V), is calculated on a two-dimensional grid in the radial plane and referenced to its minimum. At a buffer-gas temperature T, each grid point is given a weight V^{-1} that falls linearly from unity at the minimum to zero where the potential equals the thermal energy $\frac{3}{2}k_{\mathrm{B}}T$. η_{eff} is the V^{-1}-weighted average of η over this grid.

Figure 1a shows η_{eff} from 4 to 300 K for ideal and shifted 8-pole, 16-pole and 16-wire traps. At 4 K it is largest in the shifted 16-wire trap and over a factor of two smaller in the ideal 16-pole trap, and shifting the electrodes raises it in every geometry (Fig. 1b). Up to 10 K, η_{eff} rises steadily in the 8-pole and ideal 16-pole traps but first falls in the other three, the same traps in which the ion temperature deviates most from the buffer-gas temperature (Fig. 1d). At high temperatures η_{eff} increases in all traps, the ideal and shifted curves merge, and all values agree within a few per cent at 300 K (Fig. 1c).

These results link η_{eff} to trap geometry and temperature, providing a route towards estimating the ion temperature directly from the effective potential, without full trajectory simulations.

References

[1] Gerlich D 1992 *Adv. Chem. Phys.* **82** 1–176
[2] Otto R *et al.* 2009 *J. Phys. B: At. Mol. Opt. Phys.* **42** 154007

†E-mail: pragyanandansk@gmail.com

Iodine anion photodetachment in a 16-pole ion trap

Pritam Bisi[†] and S Sunil Kumar

Department of Physics, Indian Institute of Science Education and Research, Tirupati 517619, India

Synopsis We benchmark a room-temperature 16-pole radiofrequency ion trap by measuring the absolute photodetachment cross section of mass-selected iodine anions (I^-) from the photodetachment decay rate and the simulated ion column density, obtaining $(2.0 \pm 0.2) \times 10^{-17}$ cm^2 at 378 nm and $(1.7 \pm 0.2) \times 10^{-17}$ cm^2 at 403 nm. The 16-pole ion trap will be used for gas-phase photofragmentation or photodetachment of biomolecular ions and chirality-sensitive photofragmentation of enantiomers with circularly polarised light.

The absolute photodetachment cross section is a measure of the photostability of anions. A room-temperature 16-pole ion trap has been developed in our group [1], with which absolute cross sections of molecular and atomic ions can be measured within hours [2].

Anions from an electrospray source pass an ion transfer capillary, an RF ion funnel and a quadrupole ion guide, are mass-selected by a quadrupole mass filter (QMF) and stored in the 16-pole trap (figure 1). After a variable storage time they are extracted through an einzel lens and a second QMF, set to the parent or a fragment mass, onto a microchannel-plate (MCP) detector.

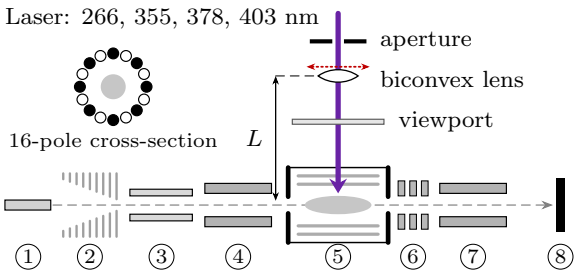

Figure 1. Setup: (1) capillary, (2) ion funnel, (3) quadrupole ion guide, (4, 7) QMFs, (5) 16-pole trap, (6) einzel lens, (8) MCP detector; L is the lens–trap distance.

Laser-on and laser-off decay curves of the ion number versus storage time give the photodetachment rate k_{pd} and the background rate k_{bg}. As $k_{\mathrm{pd}} = \sigma_{\mathrm{pd}}\,\rho(r)\,F_{\mathrm{L}}$, where F_{L} is the photon flux and $\rho(r)$ the single-particle column density at the laser position obtained from simulations of the trapped ion cloud, a single rate measurement yields σ_{pd} without full laser depletion tomography [2].

The iodine anion (I^-) is an ideal benchmark, since its only photo-induced loss is detachment. We obtain $\sigma_{\mathrm{pd}} = (2.0 \pm 0.2) \times 10^{-17}$ cm^2 at 378 nm and $(2.0 \pm 0.2) \times 10^{-17}$ cm^2 at 403 nm, in agreement with the reported values [3].

Our main goal is to probe chirality by photofragmentation. Irradiating a mass-selected enantiomer with left- or right-circularly polarised light (LCP/RCP) gives the photofragmentation cross sections σ_{L} and σ_{R} and hence the asymmetry factor $g = 2(\sigma_{\mathrm{L}} - \sigma_{\mathrm{R}})/(\sigma_{\mathrm{L}} + \sigma_{\mathrm{R}})$, a mass-resolved analogue of circular dichroism [4]. Enantiomer pairs such as D/L-tryptophan provide a built-in control: a genuine chiroptical signal reverses sign between D and L.

References

[1] Salvi M *et al.* 2023 *Rev. Sci. Instrum.* **94** 093203

[2] Mohandas S *et al.* 2025 *J. Chem. Phys.* **163** 094304

[3] Neiger M 1975 *Z. Naturforsch. A* **30** 474

[4] Daly S *et al.* 2020 *Science* **368** 1465

[†]E-mail: ritambisi20243408@students.iisertirupati.ac.in

Space-charge-limited Coulomb crystals in a 3D Paul trap: direct N-body simulation versus cold-fluid theory

V R Alagappan[1], B Govindan[2] and K T Satyajith[3†]

[1]IISER Tirupati, Jangalapalli, India
[2]Nuclear Design and Engineering, L&T Heavy Engineering, Surat, India-395007
[3]Delta Q, IMJ Institute of Research and Department of Basic Science and Humanities, Moodalkatte Institute of Technology, Moodalkatte, Karnataka 576217, India

Synopsis At fixed static voltage, a cooled Coulomb crystal in a 3D Paul trap flattens as the RF amplitude rises. Direct N-body simulations in the full RF field show its aspect ratio falling from 0.72 to 0.41 between 150 and 250 V, so its radius shrinks as $V_{\rm rf}^{-0.45}$ rather than the fixed-shape $V_{\rm rf}^{-2/3}$. A parameter-free cold-fluid model reproduces the shape to 1.5% and the radius to 1% at $N = 1000$.

Once Coulomb repulsion balances the trapping field, cold-fluid theory predicts the size and shape of a cooled ion cloud from the trap parameters alone [1]. Earlier tests compared crystal shapes with experiment and ion numbers with molecular dynamics [2]; here we test the absolute radius, aspect ratio and density against direct N-body simulations in the full RF field.

We integrate every ion in the instantaneous field of an ideal 3D quadrupole trap ($r_0 = 1$ mm, $\Omega/2\pi = 10$ MHz, $U_{\rm dc} = 5$ V), with exact Coulomb forces and no pseudopotential approximation. A Langevin thermostat [3] at the $^{40}Ca^+$ Doppler limit represents laser cooling. Clouds of $N = 10$–1000 ions start at rest at $V_{\rm rf} = 150$–300 V ($q_z = 0.37$–0.73).

At $V_{\rm rf} \le 250$ V every cloud relaxes within a few microseconds into an oblate Coulomb crystal below 0.8 mK, with $R_{\rm rms} \propto N^{0.352\pm0.004}$ (Fig. 1a).

The cold-fluid model combines the uniform density $n_0 = 3\varepsilon_0 V_{\rm rf}^2/(m\Omega^2 r_0^4)$, the spheroid shape set by the depolarisation factor [1], and RF-averaged micromotion. With no free parameters it reproduces the radius to 10% at $N = 10$ and 1% at $N = 1000$; the residual is a $V_{\rm rf}$-independent density excess of the discrete crystals (5% at $N = 200$, 1.5% at $N = 1000$).

At fixed $N = 200$ the density rises as $V_{\rm rf}^2$, but because the static voltage makes ω_z/ω_r grow with $V_{\rm rf}$, the crystal also flattens. Its measured aspect ratio falls from 0.72 to 0.41 between 150 and 250 V, within 1.5% of the model (Fig. 1b). The radius therefore falls as $V_{\rm rf}^{-0.45}$ (21.6 to 17.2 μm, within 2%), not as the fixed-shape $V_{\rm rf}^{-2/3}$. Exact Floquet secular frequencies, used instead, overestimate both.

At 300 V ($q_z = 0.73$), a cloud released from the initial distribution did not crystallise, whereas a pre-formed crystal remained cold. We are investigating the origin of this dependence on the initial state.

The flattening can be imaged directly, and the results set a baseline for space-charge frequency shifts and mixed-species crystals.

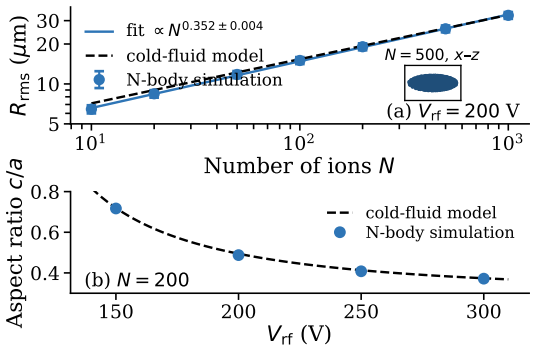

Figure 1. (a) $R_{\rm rms}$ vs N, 200 V (inset: $N = 500$). (b) Aspect ratio vs $V_{\rm rf}$, $N = 200$.

Framework co-developed with Princita Gazel Ferrao, Vandana and Vedha Varshini B [4].

References

[1] Dubin D H E and O'Neil T M 1999 *Rev. Mod. Phys.* **71** 87
[2] Fröhlich U, Roth B and Schiller S 2005 *Phys. Plasmas* **12** 073506
[3] Schneider T and Stoll E 1978 *Phys. Rev. B* **17** 1302
[4] Alagappan V R *et al.* in preparation

†E-mail: ktsatyajit@proton.me

Quekit-SDK - An Indigenous SDK for virtual trapped-ion and quantum physics simulation

Vicky Budhiraja[1†], Jitendra Verma[1], V. Ravishankar[2], and Sugam Kumar[3]

[1] QUTE Electronics, Vasant Kunj, New Delhi, 110070, India
[2] Department of Arts, Science, and Design, Indian Institute of Information Technology Dharwad, 580009, India
[3] Inter-University Accelerator Centre, New Delhi, 110067, India.

Synopsis We present Qutekit software development kit for trapped-ion quantum hardware. It provides virtual models of the main hardware used in an ion-trap experiment, such as the ion, laser, AOM, DDS, FPGA, and photon detector. A quantum program written by the user is converted into the required sequence of hardware operations. The software can be used to test these operations on a virtual system before running them on real hardware.

We have designed and developed a hardware-aware software development kit, Qutekit, for modeling various trapped-ion systems, compiling, and executing quantum programs on virtual quantum hardware. It provides virtual hardware setup capabilities, hardware chain workflows, and an execution framework in which user-level quantum instructions are translated into device-level control operations to propagate through a configurable and customisable virtual hardware stack.

The virtual hardware stack represents canonical components such as trapped-ion systems, lasers, acousto-optic modulators (AOM), direct digital synthesizers (DDS), FPGA-based timing control, and photon-detection hardware [1]. A quantum circuit given by the user is converted into a sequence of physical operations. For example, a quantum gate can be converted into laser pulses with defined frequency, phase, amplitude, and duration. The timing of these operations is also defined so that the different hardware units work in the required sequence. Ion state evolution and measurement are included in the virtual system [2]. This creates an execution path from a quantum circuit to a pulse generation sequence, ion-laser interaction, state evolution, and measurement, examined via a single Qutekit SDK framework.

The main software core of Quekit-SDK is written using a high-performance Rust core with a minimalist and simple Python interface. This enables quantum programs to be defined from Python while retaining strongly typed device models and physics-oriented execution in the underlying Rust-based SDK core.

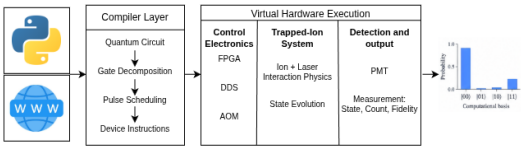

Figure 1. High-level SDK architecture diagram

The present work focuses on trapped-ion systems and provides a virtual hardware environment for developing and testing quantum control programs. The same software structure can later be connected to experimental control electronics.

References

[1] C. Lee,*Characterisation and control of trapped-ion qubit* (Ph.D.thesis, Imperial Coll., London, 2022) **10.25560/** 100200

[2] Liebfried D *et al.* 2000 arXiv:quant-ph/0009105

†E-mail: vicky@quteelectronics.com

Large associative ionization cross-section for low lying states of Li

N. Joshi[1], Vaibhav Mahendrakar[1] , M. Niranjan[1,2], Raghuveer Singh Yadav[1], E. Krishnakumar[1], A. Pandy[3], R. Vexiau[3], O. Dulieu[3], S. A. Rangwala[1,*†]

[1]Raman Research Institute, C. V. Raman Avenue, Sadashivanagar, Bengaluru 560080, India
[2]Laboratoire Charles Fabry, Institut d'Optique, CNRS, Université Paris-Saclay, 91127 Palaiseau, France
[3]Laboratoire Aimé Cotton, CNRS,
Université Paris-Saclay, Orsay, France

We observe a high rate of Li_2^+ formation via resonant excitation of ^{7}Li atoms to low-lying 2P and 3S states. It was observed in a dilute Magneto-optical trap (MOT) (average atomic separation $\approx$ 10 μm, $T \approx 500$ μK) of ^{7}Li formed at the center of a co-operational ion trap. The overlaps in the Potential Energy Curves (PECs) of neutral Li_2 and the Li_2^+, together with the quadratic dependence of Li_2^+ formation rate on the density of MOT, point towards associative ionization (AI) as the formation pathway [1]. We use the parametric excitation technique to not only identify these ions as Li_2^+ but also decipher the entire chain reaction:

$$\mathrm{Li}(3S) + \mathrm{Li}(2P) \rightarrow \mathrm{Li}_2^+ + e \rightarrow \mathrm{Li}^+ + \mathrm{Li} + e.$$

We study the photo-dissociation (PD) of Li_2^+ in the presence of MOT light. Unlike the case of Rb_2^+ [2], we observe a few long-lived Li_2^+ in the ion trap. These ions are formed in the lower vibrational states of the $X\,^2\Sigma_g^+$ PEC, which have low PD rates towards the dissociation continuum of the lowest $^2\Sigma_u^+$ state for the 670 nm wavelength. This observation offers an opportunity to co-trap Li_2^+ with other alkali species for further cold-chemistry studies. The significant AI rate of Li_2^+ suggests a large cross-section for this process. We carried out measurements to determine the AI cross-section to be very high ($\approx \pi(1000\,a_0)^2$) [1]. This is interesting, given that the participating atoms are not in high-lying Rydberg states [3].

References

[1] N. Joshi et al. 2026 *Phys. Rev. Research* **8** L032008
[2] S. Jyothi et al., 2018 *Phys. Rev. Lett.***117** 213002
[3] T. Niederprüm et al., 2015 *Phys. Rev. Lett.* **115** 013003

[†]E-mail: sarangwala@rri.res.in

Electron Impact Ionization Cross Sections and Rate Coefficients for the CS_2 Molecule

Neeraj Kumar[†]

Department of Physics, D.A.V. College, Muzaffarnagar, Uttar Pradesh, 251001, INDIA

The electron impact ionization cross section of carbon disulfide (CS_2) molecule has been evaluated systematically by using the semi-empirical Jain-Khare formalism. This approach combines quantum mechanical ideas with empirical corrections to predict ionization cross sections accurately, particularly for complex polyatomic molecules. In the present work, total ionization cross sections have been calculated over a range of incident electron energies from the ionization threshold to 1000 eV, incorporating molecular parameters such as the ionization potential, the distribution of oscillator strength, and the number of active electrons into the Jain-Khare formalism [1]. The partial ionization cross sections for the production of the main fragment ions—CS_2^+, CS^+, S_2^+, and S^+ were also obtained by incorporating appearance energies and relative yields into the model.

The results show a sharp onset of ionization cross sections at the threshold. At this threshold, the cross section rises sharply, reaching a maximum value at higher energies before gradually decreasing as the electron energy continues to increase. This trend is typical for polyatomic molecules. The agreement with experimental data [2-5] and other theoretical models [5-7] proves the accuracy and versatility of the Jain-Khare approach for total as well as fragment-specific ionization processes. These results are essential for validating models and simulating electron-driven processes in environments such as plasmas and planetary atmospheres where CS_2 is present. In addition to the evaluation of ionization cross sections, we have also calculated the ionization rate coefficients corresponding to the produced cations using the evaluated ionization cross sections and the Maxwell-Boltzmann distribution as a function of electron temperature/energy. Instead of cross sections themselves, ionization rate coefficients are more important in various plasma applications, gas discharge, and flowing after glow studies [8–9].

Neeraj Kumar gratefully acknowledges the financial support provided by the Council of Science and Technology (CST), Government of Uttar Pradesh, India, under Grant No. CST/D-821.

References:

[1] Pal S., Anshu, Kumar N., 2009, *J. Phys.* (Conf. ser.) **163,** 012030.
[2] Lindsay B. G., Rejoub R., Stebbing R. F., 2003, *J. Chem. Phys.* **118**, 5894.
[3] Rao M. V. V. S., Srivastava S. K., 1991, *J. Geophys. Res.* **96**, 17563.
[4] Freund R. S., Wetzel R. C., Shul R. J., 1990, *Phys. Rev. A* **41,** 5861.
[5] Hudson J. E., Vallance C., Harland P. W., 2004, *J. Phys. B* **37,** 445**.**
[6] Kim Y. K., Hwang W., Weinberger N. M., Ali M. A., Rudd M. E., 1997, *J. Chem. Phys.*, **106,** 1026.
[7] Vinodkumar M., Limbachiya C., Bhutadia H., 2010, *J. Phys. B* **43,** 015203.
[8] Capitelli M., Celiberto R., Cocciatore M., 1994, *Advances in Atomic, Molecular and Optical Physics*, **33**, 321—372.
[9] Fujimoto T., Semi-empirical cross sections and rate coefficients for excitation and ionization by electron collision and photoionization of Helium, *Institute of Plasma Physics Report, IIPJ-AM-8, Nagoya University, Nagoya, Japan* (1978).

[†]E-mail: drnkumarphy@gmail.com

Longitudinally Polarized Electron-Induced Ionization of Palladium Atoms: A Relativistic Spin-Asymmetry Study

Munendra Jain[†] and Sheetal Sisodiya

SVKM's NMIMS University, Indore, Madhya Pradesh, India–453112

Palladium (Pd) metal has exceptional catalytic activity and strong atomic-level interactions, making it an attractive candidate for major biomedical applications [1]. Pd atoms, in combination with other ligand molecules, have significant potential for targeted drug delivery and offer significant improvements in drug delivery systems. A docked Pd atom with any protein site can be used as a biomarker for electron microscopy due to the high scattering cross-section for the incident electron beam. Furthermore,a polarised electron beam can reveal many interesting features of the Pd atom-based nano-drug delivery system. The present study reported the spin-polarised scattering cross-section for the Pd atom in the high-energy regime. We have considered a relativistic mathematical treatment using Ehrhardt scattering geometry for inner-shell ionisation of a heavy atom(Pd) [2]. We have calculated a five-fold differential cross-section for a polarised electron beam with up-down asymmetry for k-shell ionisation under the relativistic energy regime (50 keV to 250 keV). The mathematical formulation is derived using a relativistic plane-wave Born approximation with a short-range interaction potential, and the quantum electrodynamics approach is used to account for wavefunction distortion due to the presence of a heavy nucleus. The results obtained for spin-up-spin-down asymmetry provide evidence for the fine-structure effect in the relativistic energy regime. We have observed that the applied mathematical formulation of the present study closely aligns with the experimental results under favourable conditions.

References

1. A. Dumas and P. Couvreur, *Chemical Science* **6**, 2153–2157 (2015).

2. S. Keller *et al.*, *Physical Review A* **53**, 2295 (1996).

[†]E-mail: munendra.jain@nmims.edu

Electron-impact total ionization cross sections for neutral Erythrulose $C_4H_8O_4$

Jinendra Patel[1†], Chetan Limbachiya[2] and Mohit Swadia[3]

[1]*LDRP Institute of Technology and Research, Kadi Sarva Vishwavidyalaya, Gandhinagar, 380016, Gujarat, India

[2]Department of Applied Physics, The Maharaja Sayajirao University of Baroda, Vadodara, 390002, Gujarat, India

[3]HVHP Institute of Post Graduate Studies Research, Kadi Sarva Vishwavidyalaya, Kadi, 384440, Gujarat, India

Electron-impact total ionization cross sections for neutral Erythrulose ($C_4H_8O_4$) were calculated over 11–5000 eV using the orbital-resolved Binary-Encounter-Bethe (BEB) model. The BEB orbital parameters were obtained from a pure single-point calculation at the ωB97X-D4/aug-cc-pVTZ optimized geometry. The calculated first ionization potential 10.175 eV was used for the HOMO ionization threshold. The total ionization cross section increases rapidly above threshold, reaches a broad maximum of 17.14×10^{-16} cm^2 at 87 eV and decreases smoothly at higher incident electron energies, consistent with the expected BEB energy dependence. Orbital-resolved analysis of 32 occupied molecular orbitals shows that ionization is dominated by the frontier valence region, the HOMO through HOMO-7 together contribute 51.8% of the total cross section at the peak energy. The HOMO and HOMO-1 channels individually provide 8.16% and 7.72%, respectively, of the peak cross section, demonstrating the importance of the least-bound valence electrons in electron-impact ionization of this oxygen rich molecule. In the absence of direct experimental ionization data for erythrulose, the present results provide a consistent theoretical reference dataset for future measurements and comparison with structurally related oxygenated molecules. Molecular-orbital population or visualization analysis should be used separately before assigning the frontier orbitals specifically to oxygen lone-pair or antibonding character.

References

[1] Jiménez-Serra I *et al.* 2026 *Nat. Astron.* **10** 02905
[2] Pires W A *et al.* 2017 *Int. J. Mass Spectrom.* **422** 32–41
[3] Luthra M *et al.* 2023 *Pramana* **97** 120
[4] Chai J-D and Head-Gordon M 2008 *J. Chem. Phys.* **128** 084106
[5] Kim Y-K and Rudd M E 1994 *Phys. Rev. A* **50** 3954–3967
[6] Kim Y-K *et al.* 2000 *Phys. Rev. A* **62** 052710
[7] Hwang W *et al.* 1996 *J. Chem. Phys.* **104** 2956–2966
[8] Sun Q *et al.* 2018 *WIREs Comput. Mol. Sci.* **8** e1340

†E-mail: jinendra_sh@ldrp.ac.in

K-LL Auger - Meitner emission in symmetric projectile ion - target molecule collision

Nitish Kumar[1], Rohit Tyagi[1], Manoj K. Harbola[1], Lokesh C. Tribedi[2,3] and Aditya H. Kelkar[1†]

[1]Department of Physics, Indian Institute of Technology Kanpur, Kanpur - 208016, India

[2]Department of Nuclear and Atomic Physics, TIFR, Mumbai - 400005, India

[3]R&D, UPES, Dehradun - 248007, India

Auger - Meitner (AM) electron spectroscopy is a powerful technique for studying inner-shell processes and electron - electron correlations in atomic and molecular systems. The K-LL emission provides detailed information about Auger transition probabilities, angular distributions, and post-collision interaction dynamics. In ion-atom/molecule collisions, Auger spectroscopy is especially useful for understanding target and projectile ionization mechanisms.

In this work, we report measurements of absolute double differential cross sections (DDCS) for AM electron emission from symmetric projectile - target collision system. The K-LL AM electron yields have been measured in 200 - 270 keV $C^{1,2+}$ and $N^{1,2,3+}$ collisions with CH_4 molecules. Angular distributions of Auger electrons were studied over emission angles from 30° to 150° and show nearly isotropic behavior [1]. The appearance of target and projectile AM peaks in the electron spectra were further investigated by calculating the AM transition rates. The calculations were performed using non-relativistic screened hydrogenic and Hartree - Fock wave functions. The Gordon wave function for the emitted electron shows better agreement with experimental results compared to the free-particle wave function. Measured Doppler shifts for both target and projectile emissions are in good agreement with calculated values.

As part of our current work, we are calculating Auger transition rates using newly generated wavefunctions obtained from the Kohn–Sham potential [2]. These wavefunctions are expected to provide improved descriptions of the excited-state energy levels. In parallel, we are planning to investigate Auger–Meitner (AM) processes using a higher-charge-state projectile ion, such as C^{3+} to investigate whether electron capture by the projectile is followed by Auger–Meitner decay of the excited projectile state.

In the near future, we plan to extend this work through theoretical calculations and experimental studies using a charge state analyzer (CSA), focusing on post-collision processes such as electron capture cross sections of charged projectile ions and Auger electron emission from charged projectiles.

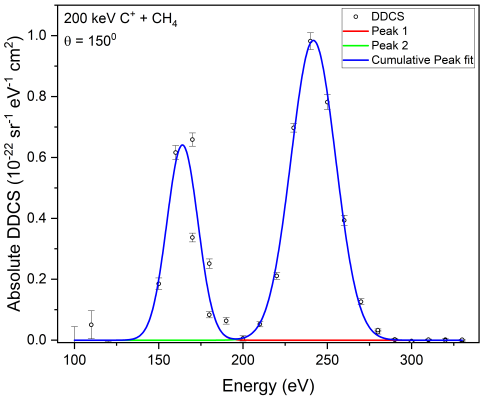

Figure 1. Target and projectile K-LL AM peaks in 200 keV C^{1+} collision with CH_4.

References

[1] Tyagi R. *et al.* 2023 *J. Electron Spectrosc. Relat. Phenom.* **269** 147407

[2] Singh P. *et al.* 2021 *Oxford Open Materials Science* **1** 1

†E-mail: akelkar@iitk.ac.in

Electron and Ion Radiation Processes on Astrophysical Ice Surfaces: Development of a New Experimental Facility at SINP, Kolkata, India

Sankhabrata Chandra[1†]

[1]Nuclear Atomic and Particle Physics Division (NAPPD) Saha Institute of Nuclear Physics (SINP) 1/AF, Bidhan Nagar, Kolkata 700064, India

Understanding the processes induced by electrons and ions on surfaces is a fascinating area of study within atomic and molecular physics. Astrophysical environments are immersed in high-energy electron and ion radiation. For example, cosmic rays (MeV to GeV) and local stellar radiation irradiate interstellar dust clouds; solar wind, low-energy (keV) electrons, and protons bombard solar system bodies; Jupiter's and Saturn's local magnetospheric trapped energetic particles such as H+, O+, S+, and He+ with keV to MeV energies are constantly bombarding Jupiter and Saturn's moons. Therefore, understanding the radiation processes on astrophysical dust ice and planetary surfaces at extreme conditions is necessary. However, studying ion- and electron-induced processes at particularly low temperatures presents unique experimental challenges such as maintaining interstellar conditions in a laboratory environment. These studies also aim to understand the origin of prebiotic species and their evolution from dense molecular clouds to planetary systems via protoplanetary disks. The primary objective of the laboratory is to explore the electron- and ion-induced processes on astrophysical dust ice surfaces to understand physical processes such as sputtering of surface species and modifications of surface species during radiation processes in the context of fundamental molecular physics, astrophysics, and planetary science. This will be studied using mass spectrometry and near- to mid-infrared spectroscopy during electron and ion irradiation, as well as during the warming of the sample using temperature-programmed desorption following electron and ion bombardment. Currently, at SINP, I am establishing the APRIS Laboratory —Astrophysical and Planetary Radiation-Ice Surface Laboratory. This will be a state-of-the-art laboratory dedicated to investigating electron- and ion-induced processes on astrophysical ices. The laboratory will provide a platform for studying fundamental physical processes under space-relevant conditions and will contribute to different areas of space science, including astrophysics and planetary science. In this presentation, I will discuss the current development of the APRIS Laboratory and its potential contributions to India's space missions, particularly ISRO missions, as well as to international space missions, including missions led by NASA and ESA.

[†]E-mail: sankhabrata.chandra@saha.ac.in

Electron-induced x-ray emission from thick Pb and Pt targets: Experimental measurements and PENELOPE simulations

Kailash Verma[1†], Namita Yadav[1], Hitesh Rahangdale[2], Suman Prajapati[1], Kumar Ankit Upadhayay[1], Raj Singh[4], Rajneesh Kumar[1]

[1] 1Department of Physics, Banaras Hindu University, Varanasi-221005
[2] S R University, Anant Sagar, Warangal, Telangana-506001
[3] Central University of Jharkhand, Ranchi- 835222
[4] Physical Sciences, IUCTE, Banaras Hindu University, Varanasi-221005

When energetic electrons interact with solid materials, a variety of atomic processes can occur, including inner-shell ionization, bremsstrahlung emission, electron backscattering, characteristic K- and L-shell X-ray production, and secondary-electron emission [1, 2]. Electron-induced X-ray emission provides valuable information about the atomic structure of matter and has applications across several areas of science and technology. In this work, X-ray emission from thick Pb and Pt targets has been experimentally investigated using electron beams in the energy range of 10–30 keV. The L-subshell X-ray production cross sections of Pb ($Z = 82$) were determined for electron energies of 15–30 keV, while the bremsstrahlung yield from Pt ($Z = 78$) was measured for incident electron energies between 10 and 25 keV using a thick-target configuration [3].

A monoenergetic electron beam was directed onto solid targets with a thickness of approximately 0.1 mm, resulting in the production of both characteristic and continuous X-ray radiation. The emitted X-rays were recorded using a Si-PIN diode detector [4], and the acquired spectra were processed and analyzed using multichannel analyzer (MCA) software. The experimental measurements were compared with results obtained from PENELOPE Monte Carlo simulations as well as with previously published experimental data. The measured total production cross section for the Lℓ line of Pb under electron impact is reported, to the best of our knowledge, for the first time. The experimental findings exhibit good consistency with the corresponding simulation results.

References

[1] Verma K, Rahangdale H, Upadhayay K A, Singh R, Singh B, and Yadav N *J. Electron. Relat. Phenom.* **280** 147541 (2025).
[2] Verma K, Singh B, Prajapati S, Singh R, and Kumar R *Appl. Radiat. Isot.* **212** 112393 (2025).
[3] Tian L X, Dai C C, Fang B B, and Liu Y J *Nucl. Instrum. Methods Phys. Res., Sect. B* **471** 84 (2020).
[4] Yadav N, Bhatt P, Singh R, Llovet X, and Shanker R *J. Electron Spectrosc. Relat. Phenom.* **185** 23 (2012).

[†]E-mail: kailash433@bhu.ac.in

Study of electron impact ionization and excitation cross sections of beryllium isoelectronic sequence

Ravin Kumar[1,†] **and G Purohit**[1,†]

[1]Department of Physics, University College of Science, Mohanlal Sukhadia University, Udaipur, Rajasthan, 313001, India

Synopsis Collisions involving electrons with atoms and molecules are one of the most fundamental interactions in physics. These interactions are basic to a variety of processes such as plasma physics [1], radiation physics, and astrophysics [2]. Electron- impact (EI) is also the most common form of ionization in commercial mass spectrometers and is used as an analytical tool for measuring species concentrations in gaseous samples.

In the present study, we have calculated electron impact ionization and excitation cross sections of beryllium isoelectronic sequence such as B^{+}, C^{2+}, N^{3+}, O^{4+}, F^{5+} and Ne^{6+} by employing Distorted Wave (DW), Binary Encounter Dipole (BED), and Coulomb-Born Exchange (CBE) approaches employed in the flexible atomic code [3] and compared with the available theoretical and experimental results.

Theoretical methods: Ionization cross sections of the beryllium isoelectronic sequence (as B^{+}, C^{2+}, N^{3+}, O^{4+}, F^{5+} and Ne^{6+}) are computed using the DFS method used in the FAC [3].

The electron ionization processes is described using the DW, CBE and BED approaches. The required bound and continuum wave functions for every ion are produced using the local central potentials for the ground configurations.

Relativistic Distorted Wave theory: The direct ionization cross section from initial state to a final state can be expressed as

$$\sigma_{01} = \frac{\pi}{k_0^2 g_0}\Omega_{01}$$

Where g_0, is the statistical weight of the initial state and k_0 is the kinetic momentum of the incident electron.

Coulomb-Born Exchange approach: By using the CBE approximation, cross sections have also been computed. In comparison to the DW method, this approach computes radial integrals more quickly. In the CBE approximation, reduced radial integrals obtained are not sensitive and, in that approximation, hydrogenic values have been used in place of DW radial integrals. While in DW method fitting parameters are used to calculate total ionization cross sections at different enrgies.

Binary Encounter Dipole Theory: The total ionization cross sections (TICS) have been obtained by integrating the above equation which can be written as,

$$\sigma_i(t) = \int_0^{(t-1)/2} \frac{d\sigma}{d\omega} d\omega$$

$$\sigma_i(t) = \frac{S}{t+u+1} \left[D(t)\ln t + \left(2 - \frac{N_i}{N}\right)\left(1 - \frac{1}{t} - \frac{\ln t}{t+1}\right)\right]$$

A unique quality of the BED theory is the energy denominator, which reduces the ionization cross sections at low energies. When the experimental and theoretical results compared for the low Z ions are found reasonable agreement by introducing such scaling factor.

References

[1] A. Müller, *Adv. At. Mol. Opt. Phys.*, **55**, 293-417. (2008).
[2] T.R. Kallman, P. Palmeri, *Review of Modern Physics*, **79**, 79-133 (2007).
[3] M. F. Gu, flexible atomic code, *J. Can. Phys.* (2008).

[†]E-mail: rvin19101994@gmail.com
[†]E-mail: gvpurohit1974@gmail.com

Laboratory Simulation of Titan's Ionospheric Conditions

Abhina K P [†], Antony Arupara, Malavika S, Shravan Kale, Umesh R Kadhane [†]

Atomic and Molecular Physics Laboratory, Indian Institute of Space Science and Technology, Thiruvananthapuram, Kerala 695547, India

Synopsis RF driven plasma of nitrogen-methane mixture is used to recreate molecular processing in the ionosphere of Titan. While stable molecules produced during this plasma processing were monitored in real-time using mass spectrometry, the resulting Tholin deposition on different substrates were investigated using SEM, and mass spectra were recorded during plasma operation. Further work will focus on experiments with condensation of volatiles produced as well as direct extraction of boh positive an negative ions from the plasma reactor.

Titan, Saturn's largest moon, has a nitrogen-rich atmosphere containing methane. Solar radiation and energetic particles from Saturn's magnetosphere initiate ionization, dissociation, and chemical reactions that lead to the formation of complex organic compounds. These compounds contribute to the formation of aerosols known as *tholins*, which serve as laboratory analogues for investigating the chemistry of Titan's atmosphere[1]. Understanding how these materials form and identifying the chemical species involved are important for studying the evolution of organic matter in planetary atmosphere.

In this study, a nitrogen–methane plasma was generated using a 13.56 MHz radio-frequency inductively coupled plasma (RF-ICP) source to simulate aspects of Titan's atmospheric chemistry. Tholin deposited during plasma operation was collected on three substrates: silicon (Si), fluorine-doped tin oxide (FTO), and quartz. The samples were examined using scanning electron microscopy (SEM), and the images were compared with those of the corresponding uncoated substrates. The SEM images revealed an additional surface layer on the plasma-exposed samples that was absent in the uncoated substrates, providing morphological evidence of deposition. Using three different substrates also allows the deposited material to be examined on different surface types. Further characterization will be carried out to investigate the morphology, composition, and chemical properties of the deposited tholin.

Mass spectra were also recorded during nitrogen–methane plasma operation to investigate the molecular species formed through plasma-induced chemical reactions. Signals were observed at mass-to-charge ratios (m/z) above 50, indicating the presence of species across a broad mass range. These measurements provide an initial basis for investigating the chemical products formed in the plasma and developing a more complete understanding of plasma-driven organic chemistry.

Further experiments are planned using a liquid-nitrogen cold trap to collect condensable reaction products for subsequent analysis. A new plasma reactor model is also being developed to improve the direct sampling of neutral species, positive ions, and negative ions while minimizing disturbances to the plasma. Together, these studies aim to investigate the gas-phase products and deposited organic materials produced during nitrogen–methane plasma reactions.

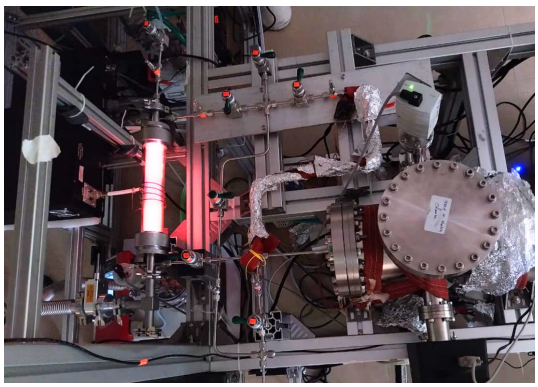

Figure 1. Experimental setup used for the laboratory simulation.

References

[1] Sciamma-O'Brien E *et al.* 2014 *Icarus* **243** 325–336

[†]E-mail: corresponding. abhinakattungal@gmail.com
[†]E-mail: corresponding. umeshk@iist.ac.in

Modelling Plasmon Excitations in Planar PAH Systems

Arjun Jaikrishna M[1†], **and Umesh Kadhane**[1†]

[1]Atomic and Molecular Physics Laboratory, Indian Institute of Space Science and Technology, Thiruvananthapuram, Kerala 695547, India

Synopsis We develop an analytical hydrodynamic model to investigate collective electronic excitations in PAH-inspired molecular systems. Using a jellium-based cylindrical shell geometry, we derive the bulk and surface charge-density modes, revealing multiple coupled surface plasmon branches arising from the system' s finite boundaries. This framework provides insight into the role of confinement and geometry in shaping molecular-scale collective excitations.

Collective excitations arise in a wide range of physical systems, from atomic nuclei, where they manifest as giant resonances such as the giant dipole resonance (GDR), to condensed-matter systems, where the coherent oscillations of delocalized electrons are known as plasmons [1–3]. These electronic excitations can couple strongly to electromagnetic radiation, giving rise to characteristic resonant responses. While plasmons are well established in bulk metals and metallic nanostructures, they have also been identified in finite carbon-based systems, including C60 fullerenes and polycyclic aromatic hydrocarbons (PAHs) [4, 5].

In PAHs, absorption features in the 17–18 eV energy range have been associated with molecular plasmon resonances, with reported absorption cross sections reaching 25 Mb–35 Mb per carbon atom [5]. The characteristics of these excitations depend on the size and topology of the molecule, motivating theoretical investigations of collective electronic behavior in finite, confined systems.

Plasmon resonances can be studied using different theoretical approaches, ranging from the classical Drude model to microscopic methods such as the random phase approximation (RPA) and time-dependent density functional theory (TDDFT) [6]. While these approaches describe collective electronic excitations at different levels of detail, their computational cost and treatment of nonlocal effects vary. The hydrodynamic model provides an intermediate approach, treating electrons as a continuous fluid while incorporating pressure effects and spatial dispersion [7]. In this work, we employ this model to investigate collective electronic excitations in planar molecular systems.

The model considers the system to be a finite cylindrical shell of electron gas within the jellium approximation, enabling the effects of confinement and boundary geometry to be treated analytically. Starting from the linearized hydrodynamic equations, we derive the governing equations for bulk and surface charge-density oscillations. The resulting formulation separates volume and boundary contributions to the induced charge density and yields a coupled set of equations for the surface modes. The model predicts a bulk plasmon mode at the characteristic plasma frequency, $\omega_p = \sqrt{4\pi\rho_0}$, alongside multiple coupled surface plasmon branches associated with the cylindrical and planar boundaries of the system.

This analytical framework provides a basis for investigating how confinement and boundary geometry shape collective electronic excitations in PAH-inspired molecular systems and related finite carbon nanostructures.

References

[1] Ishkhanov BS, Kapitonov IM. 2021 *Phys. Usp.* **64** 141–156
[2] Lauchner A *et al.* 2015 *Nano Lett.* **15** 6208–6214
[3] Pines D, Bohm D. 1952 *Phys. Rev.* **85** 338–353
[4] Bertsch GF, Bulgac A, Tom'anek D, Wang Y. 1991 *Phys. Rev. Lett.* **67** 2690–2693
[5] Hróðmarsson H *et al.* 2025 *Astron. Astrophys.* **698** A202
[6] Varas A, García-González P, Feist J, García-Vidal FJ, Rubio A. 2016 *Nanophotonics* **5** 409–426
[7] Verkhovtsev A, Korol AV, Solov'yov AV. 2012 *Eur. Phys. J. D* **66** 253

†E-mail: arjunjaikrishna0604@gmail.com
†E-mail: umeshk@iist.ac.in

Fragmentation dynamics of exotic ionic species derived from the toluene cation under CID

B Panja[1†], M Arjun Jaikrishna[1], A Antony[1], J Rejila[1], U Kadhane[1†]

[1]Atomic and Molecular Physics Laboratory, Indian Institute of Space Science and Technology, Thiruvananthapuram, Kerala 695547, India

Synopsis This study covers the dissociation dynamics of toluene cations. Moreover, it extends beyond the ionization and dissociation of toluene to probe the subsequent fragmentation of the ionic species it produces. Energy-correlated time-of-flight measurements establish precursor–product correlations, revealing new fragmentation channels and reassessing previously proposed pathways of the toluene ion.

The fragmentation dynamics of the toluene molecular ion are examined as a function of internal energy using 266 nm multiphoton ionization (MPI) and energy-correlated time-of-flight mass spectrometry, complemented by electron-impact ionization (EI). Under MPI, H loss is observed as the intense primary fragmentation channel. Its pronounced abundance points to an alternative ionization pathway beyond the conventional sequential multiphoton ionization picture, while comparison with EI provides additional insight into the energy dependence of the fragmentation.

Energy-correlated time-of-flight measurements performed under this study establish precursor–product relationships for primary and secondary fragmentation channels, revealing losses of C_4H_3, C_4H_4, and C_4H_5 that are not readily resolved in conventional mass spectra. Several competing pathways are found to converge on the same $m/z = 51$ product ion, revealing multiple routes to its formation. Under collision-induced dissociation (CID), the formation of $m/z = 89$ is identified as H_2 loss from $m/z = 91$, rather than H loss from $m/z = 90$, demonstrating the ability to distinguish competing dissociation pathways and identify preferential H_2 elimination.

The combination of MPI and subsequent CID further enables the fragmentation behaviour of reactive ionic species produced from toluene to be probed as a function of internal energy, even when these species are not readily available as standalone ions. Together with density functional theory (DFT) calculations, the measurements provide an interconnected fragmentation network and identify previously unrecognized pathways. The resulting products include $C_7H_7^+$, $C_6H_5^+$, $C_5H_5^+$, $C_4H_4^+$, $C_4H_3^+$, $C_4H_2^+$, and $C_3H_3^+$. These reactive hydrocarbon ions are of astrochemical interest because ion–molecule reactions can promote the growth of larger hydrocarbon ions and polycyclic aromatic hydrocarbons (PAHs), contributing to the chemical complexity of planetary atmospheres and interstellar environments [1–3].

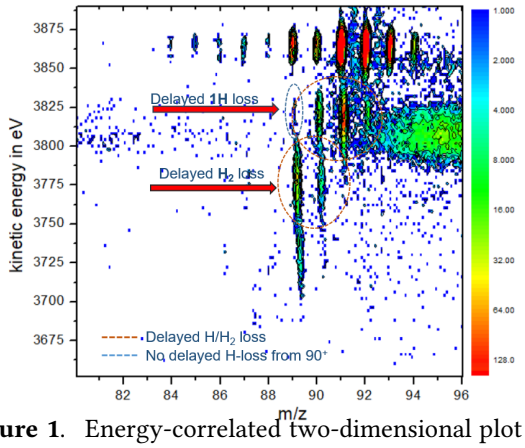

Figure 1. Energy-correlated two-dimensional plot of toluene in the $m/z = 94$–84 range, illustrating the progression of H- and H_2-loss fragmentation under MPI–CID.

References

[1] McEwan M J and Anicich V G 2007 *Mass Spectrom. Rev.* **26** 281–319.
[2] Westlake J H *et al.* 2015 *J. Geophys. Res.: Space Phys.* **120** 8018–8036.
[3] Sandford S A *et al.* 2020 *Chem. Rev.* **120** 4616–4659.

†E-mail: bindujapanja24@gmail.com
†E-mail: rkumesh@gmail.com

Pyridine under Electron-Impact and Multiphoton Ionisation: Estimation of Appearance Energies and Identification of Dissociation Pathways

Devika V S[1†], Binduja Panja [2], Arupara Antony Joseph [2], Arjun Jaikrishna [2], Dhanvi Anu [1], Rejila J [2], Ria Sankaranarayanan [1], Murugadass K [1†], Umesh R Kadhane [2†]

[1] Amrita School of Physical Sciences, Amrita Vishwa Vidyapeetham, Coimbatore, 641112, India.

[2] Atomic and Molecular Physics Laboratory, Indian Institute of Space Science and Technology, Thiruvananthapuram, 695547, India

Investigating the fragmentation dynamics of nitrogen-containing aromatic molecules provides insights into sequential hydrogen loss, thereby strengthening our understanding of their chemistry in astrochemical environments. Pyridine, a nitrogen-containing aromatic heterocycle relevant to both biological chemistry and astrochemistry, provides a useful model system for investigating ionisation-induced fragmentation [1]. In this work, the fragmentation dynamics of pyridine are investigated using electron-impact ionisation (EI) and multiphoton ionisation (MPI), focusing on appearance energies, sequential hydrogen loss, and competing dissociation pathways.

Mass spectra obtained under EI and MPI reveal sequential hydrogen loss from the pyridine molecular ion (m/z 79), producing fragments spanning m/z 78−74. Electron-energy-dependence measurements are used to determine the appearance energies of prominent fragments and examine their energy-dependent formation [2]. Notably, the m/z 77 and 76 signals exhibit similar onset regions, although the latter increases more rapidly with electron energy. These observations indicate sequential hydrogen loss, with the m/z 77 ion undergoing further dehydrogenation to form the m/z 76 ion. Density functional theory (DFT) calculations will be used to evaluate the structural stability of both ions and the energetic feasibility of this fragmentation pathway. Comparing the calculated energy requirements with experimental appearance energies will help assess the feasibility of this process. Previous studies have also demonstrated the complexity of pyridine fragmentation, including HCN and HNC loss, highlighting the importance of theoretical investigations in understanding its dissociation mechanisms [2].

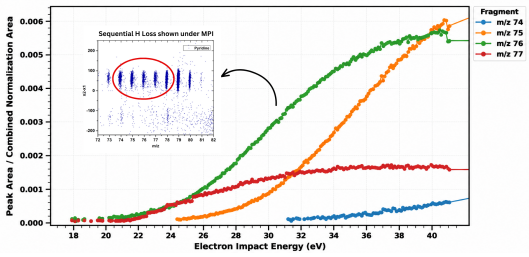

Figure 1. Electron Energy Dependence plot of pyridine showing the sequential H loss under EI along with the 2D Energy Correlation plot under MPI

The combined experimental and theoretical investigation provides insights into the sequential hydrogen-loss series from the pyridine parent ion (m/z 79) to the fragments at m/z 78−74, as well as the energy-dependent fragmentation of pyridine under EI and MPI. This study contributes to a better understanding of fragmentation processes in nitrogen-containing aromatic molecules relevant to astrochemical environments.

References

[1] Mondal S, Wouterlood B, Garcia G A, Nahon L, Stienkemeier F and Hartweg S 2026 *Phys. Chem. Chem. Phys.* **28** 17361–17370

[2] Jurkowski M K, Wasowicz T J 2023 *Rom. J. Phys.* **68** 205

[3] Rap D B, Simon A, Steenbakkers K, Schrauwen J G M, Redlich B and Brünken S 2023 *Faraday Discuss.* **245** 221–244

†E-mail: vsdevika24@gmail.com
†E-mail: k_murugadass@cb.amrita.edu
†E-mail: umeshk@iist.ac.in

Appearance Energy of Benzonitrile Fragment Cations Under Low Energy Electron Impact

Dhanvi Anu[1†], Devika V S[1], Ria Sankaranarayanan[1], Binduja Panja[2], Rejila J[2], Arjun Jaikrishna M[2], Umesh R Kadhane[2†] and Murugadass K[1†]

[1]Amrita School of Physical Sciences, Amrita Vishwa Vidyapeetham, Coimbatore, 641112, India.

[2]Atomic and Molecular Physics Laboratory, Indian Institute of Space Science and Technology, Trivandrum, 695547, India

Synopsis Dissociative ionisation of benzonitrile (C_6H_5CN) is studied under low-energy electron impact to map the energy dependence of its various dissociation channels. Instrument-specific appearance energies ranging from 14.8 to 23.7 eV were estimated for all prominent primary and secondary channels. An attempt is made to correlate the variation in appearance energy with isomerisation, the sequence of dehydrogenation, ring opening and the formation of cyanopolyynes cations.

Cold interstellar clouds such as TMC-1 are rich in nitrogen-bearing molecules, the most abundant of which are the cyanopolyynes ($HC_{2n+1}N$). The same cloud also hosts benzonitrile (C_6H_5CN), the first aromatic ring detected by radio astronomy [1]. Threshold coincidence studies indicate that the benzonitrile radical cation dissociates through many parallel channels, yielding fragments such as HC_3N [2]. However, the complete fragmentation network, including the order in which the channels open and how they are interconnected, has not yet been fully established. In this work, we investigate the dissociative ionisation of benzonitrile by electron impact, using appearance energy measurements to identify the fragmentation channels and determine their onsets.

Electron impact ionisation often leaves the target molecular species in an ionized as well as internally excited state. This internal energy then governs the statistical disassociation process in the parent cation. When this transfer exceeds the ionisation energy, a molecular ion is formed, and any energy beyond that is retained as internal excitation that can drive fragmentation. Tuning the electron energy from 11 to 30 eV controls which fragmentation channels. The yield of each ion as a function of electron energy was recorded and used to determine its appearance energy.

The appearance energy (AE) of a fragment ion is the lowest energy at which it is observed in an experiment, whereas the threshold energy is the true, instrument-independent minimum energy required to form that fragment. Therefore, over and above the threshold energy, additional instrument-specific internal energy, called the kinetic shift, is required to make the decay product ions observable in a given setup. Thus, it can safely be assumed that AE ≈ TE + kinetic shift. This distinction is important for benzonitrile because its channels differ in mechanism.

AEs were obtained for fragment ions from *m/z* 26 to 102. The parent ion (*m/z* 103) appears at 11 eV. The lowest AEs correspond to *m/z* 76 (14.8 eV) and *m/z* 77 (15.3 eV). Several fragments follow an unexpected order in which the more dehydrogenated ion appears at lower energy than the less dehydrogenated one: *m/z* 101 (17.7 eV) before *m/z* 102 (18.9 eV), *m/z* 63 (16.6 eV) before *m/z* 64 (17.8 eV) and *m/z* 65 (18.1 eV). In addition, the *m/z* 75 curve shows two kinks, indicating two formation routes: directly from the parent ion, and by H loss from *m/z* 76 also stating one of the structure is cyclic and the other is linear.

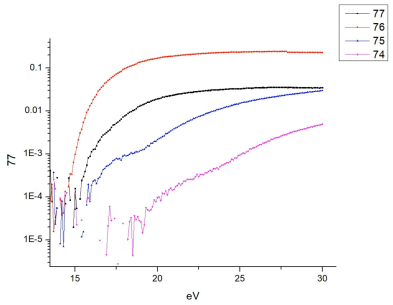

Figure 1. The m/z 75 ion (HC_5N^+, a cyanopolyyne cation) shows a double kink, indicating two formation pathways.

References

[1] Kamer J *et al.* 2023 *Phys. Chem. Chem. Phys.* **25** 29070
[2] Rap D B *et al.* 2023 *Faraday Discuss.* **245** 221
[3] Bou Debes D *et al.* 2025 *Astron. Astrophys.* **693** A304

†E-mail: anudhanvi2003@gmail.com
†E-mail: umeshk@iist.ac.in
†E-mail: dass.phy@gmail.com

Energy resolution and absolute efficiency calibration facility for Low-energy plasma sensor for Venus Mission

Malavika S [†], Rejila J, Shravan Kale, Jaimin Chaudhari, Rohit Kumar, Umesh R Kadhane [†]

[†] Atomic and Molecular Physics Laboratory, Indian Institute of Space science and Technology, Thiruvananthapuram, Kerala-695547, India

Synopsis Development of an automated ground calibration system for the RPA payload for the upcoming Venus mission. The facility is designed to satisfy the need to produce a well defined energy and intensity distribution low energy ions and electrons using electron impact ionization and VUV photo-ionization of inert gas target.

A Retarding Potential Analyzer (RPA) is a plasma diagnostic instrument used to measure the energy distribution of charged particles and determine plasma parameters such as ion and electron density, temperature, and flow characteristics. RPAV is designed to investigate the plasma environment of Venus, with a particle concentration measurement range of 10–10^6 cm^{-3}.

The system will characterize ion and ionospheric electron populations at 100−5000 K and solar-wind electrons at 25,000–500,000 K. Accurate low-energy measurements require calibration for thermal dimensional changes, magnetic-field interference, secondary-electron contamination, and grid misalignment, which affect particle transmission and energy resolution.

A dedicated ground calibration system is being developed to characterize the RPA's energy response, transmission efficiency, density response, and secondary-electron effects under controlled vacuum conditions. Measured current–retarding potential characteristics will be fitted with appropriate particle-distribution models to determine energy distributions and derive plasma parameters, including temperature and density, ensuring reliable measurements through instrumental-response calibration.

An inert gas will be introduced into a localized interaction region through a slit-jet mechanism. Electron-impact and VUV photo-ionization will generate charged particles with well-characterized energy distributions. The VUV source must provide a focused photon flux of at least 10^{11} photons $s^{-1}\,mm^{-2}$,with a beam diameter below 0.5 mm at a distance of approximately 10 cm or greater, for energy calibration. An electron source operating at 100 eV–10 keV, with an energy spread of approximately 0.5 eV and adjustable beam current of 10 nA–100 µA, will provide higher particle fluxes for density calibration. Extractor grids on both sides of the interaction region will direct electrons and ions towards the sensor.

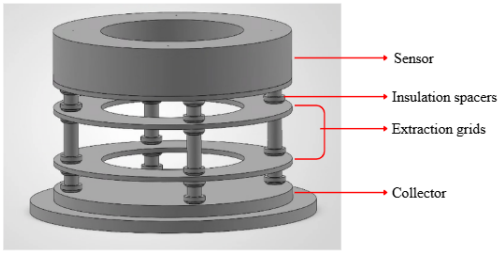

Figure 1. Grid arrangement for ion,electron extraction.

Gas-flow simulations and SIMION-based electrostatic particle-trajectory simulations are being conducted to optimize gas injection, extraction geometry, beam profiles, and particle transmission. The system will incorporate automated control and data acquisition to facilitate systematic characterization of the instrumental response of RPAV and support reliable and frequently reproducible low-energy plasma measurements for Venusian ionospheric investigations.

References

[1] Knudsen W C *et al.* 1980 *IEEE Trans. Geosci. Remote Sens.* **18** 54–59

[2] Denieffe K, Mahony C M O, Maguire P D, Gahan D and Hopkins M B 2011 *J. Phys. D: Appl. Phys.* **44** 075205

[†]E-mail: corresponding. malavikask1810@gmail.com
[†]E-mail: corresponding.umeshk@iist.ac.in

In search of evidence of plasmon excitation in PAHs at low-energy electron impact

Ria Sankaranarayanan[1†], Arjun Jaikrishna M[2], Binduja Panja[2], Devika VS[1], Dhanvi Anu[1], Umesh R Kadhane[2†] and K Murugadass[1]

[1] Amrita School of Physical Sciences, Amrita Vishwavidyapeetham, Coimbatore, Tamil Nadu 641112, India

[2] Atomic and Molecular Physics Laboratory, Indian Institute of Space Science and Technology, Thiruvananthapuram, Kerala 695547, India

Synopsis Plasmon excitation in polycyclic aromatic hydrocarbons (PAHs) is well established for fast charged particles, but it has so far been inferred only indirectly, from statistical fragmentation patterns. We report the first successful attempt to extract the effects of plasmon excitation in PAHs under electron impact at energies comparable to the plasmon energy (about 17 eV).

Plasmon (collective) excitations are coherent oscillations of the delocalized, less tightly bound electrons of a system. They appear in metal clusters, graphite, fullerenes and polycyclic aromatic hydrocarbons (PAHs), and even in nuclei [1,2]. In a plasmon, the electron density oscillates collectively relative to the positive ionic background, giving rise to a characteristic plasmon frequency [1,2]. Plasmon excitation has a very large cross section, and its oscillator strength is much greater than one, which is itself a signature of a collective excitation [3]. A plasmon resonance occurs when the energy deposited matches this characteristic energy and drives it into a higher energy state. Depending on the energy retained it either decays by autoionization [1,2] or if it is high enough, it redistributes the excess energy over all the vibrational modes of the ion, which then dissociates statistically [1,3].

Charged particles can transfer a wide range of energies in a single collision, and their strong electric fields give rise to large ionization cross sections [1] when compared to the case of photoionization. For planar aromatic molecules the plasmon peak lies at about 17 eV [1,2] with a half-width of about 7–8 eV [2], and the photoionization cross section is about 22 Mb per carbon atom [4].

Plasmon excitation by fast charged particles has been studied by colliding high energy protons with naphthalene. The yields of H and C_2H_2 loss stayed nearly constant as the proton energy changed, and a comparison with photon-induced breakdown curves indicated an energy deposition of about 18 eV and attributed to plasmon excitation [2].

In this work, we measured the yields of the fragment ions of azulene and naphthalene (both $C_{10}H_8$) as a function of electron impact energies around the plasmon resonance energy. Each yield curve was smoothed and differentiated. For azulene, the derivatives of the H-loss ($C_{10}H_7^+$, m/z 127) and C_2H_2-loss ($C_8H_6^+$, m/z 102) channels, which are linked to plasmon decay [3], peak at about 17 eV with a spread of about 6–7 eV, close to the plasmon energy and width of PAHs [2]. The derivative of the $2H/H_2$-loss channel ($C_{10}H_6^+$, m/z 126) peaks well above the plasmon energy range, pointing to a different excitation process. Furthermore, a similar treatment of other fragmentation channels reveal more complex behavior. These aspects are being explored in the context of fundamental charged particle interactions with molecules and its astrophysical implications.

References

[1] Vinitha M V *et al.* 2018 *J. Chem. Phys.* **149** 194303
[2] Mishra P M 2014 PhD thesis, Indian Institute of Space Science and Technology, Thiruvananthapuram
[3] Najeeb P K 2017 PhD thesis, Indian Institute of Space Science and Technology, Thiruvananthapuram
[4] Hrodmarsson H R *et al.* 2025 *Astron. Astrophys.* **698** A202

[†]E-mail: mailtoria05@gmail.com
[†]E-mail: umeshk@iist.ac.in

Proposal for the Direct Measurement of the Zero-Point Energy

Tufail Khan[1†], Pallavi[4], Avnish Ola[3], Veena C.P.[1], Kedar Mal [1], C.P. Safvan [1], W. Quint[2], M. Vogel[2], and Sugam Kumar[1]

[1]Inter-University Accelerator Centre, Aruna Asaf Ali Marg, New Delhi 110067, India

[2]GSI Helmholtzzentrum für Schwerionenforschung, Planckstraße 1, 64291 Darmstadt, Germany

[3]University of Delhi, New Delhi, India

[4]Jawahar Lal Nehru University, New Delhi, India

Synopsis We propose a direct measurement of the electron zero-point energy through photodetachment of trapped H^- ions. In a magnetic field, the detached electron occupies quantized cyclotron states, shifting the lowest threshold by $\hbar\omega_+/2$. Progress on trap commissioning, ion production,trapping and detection using CEM through time of flight technique is reported.

The non-zero ground-state energy of the quantum harmonic oscillator, $E_0 = \hbar\omega/2$, is a fundamental consequence of quantum mechanics. We propose a direct measurement of electron's zero point energy using laser photodetachment of H^- anions confined in a Penning trap [1]. The detached electron remains confined by the trap fields rather than entering a three-dimensional free-particle continuum, so that the lowest threshold is shifted, to leading order, to $h\nu_{\rm th} = E_{\rm A} + \hbar\omega_+/2$, where $E_{\rm A}$ is the hydrogen electron affinity and ω_+ is the reduced cyclotron frequency. Magnetic-field-dependent threshold shifts associated with the electron cyclotron zero-point energy have previously been observed in negative-ion photodetachment [2].

We report progress toward implementing this scheme with the Delhi Penning Trap (DPT) at the Inter-University Accelerator Centre, New Delhi. For the proposed zero-point-energy measurement, operation of the cryogenic trap within a 1 T superconducting magnet is proposed. Its open geometry provides particle injection, extraction and optical access, related open-access cylindrical Penning-trap concepts have been developed for precision experiments [3].

Commissioning has established electron-gun ion production, trapping, extraction and time-of-flight detection using a channel electron multiplier (CEM). The detection and data-acquisition chain is being optimized for stable ion counting and reproducible measurement cycles.

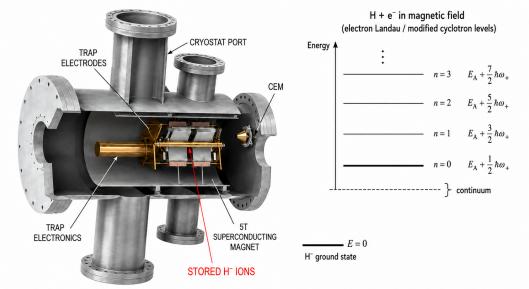

Figure 1. Proposed cryogenic Penning-trap configuration in a 5 T superconducting magnet and Landau levels of the detached electron and the zero-point shifted photodetachment threshold.

The next steps are reliable production and confinement of H^- ions, narrow-linewidth laser scans across the photodetachment threshold and controlled counting of the photodetachment products. Systematic effects relevant to the threshold resolution are being evaluated, including ion temperature, motional broadening, Zeeman structure, magnetic-field inhomogeneity, electrostatic anharmonicity and final-state interactions. These developments define the experimental requirements for resolving the zero-point contribution through precision threshold spectroscopy.

References

[1] Kumar S, Quint W and Vogel M 2025 *J. Phys. B: At. Mol. Opt. Phys.* **58** 245002
[2] Larson D J and Stoneman R 1985 *Phys. Rev. A* **31** 2210–2214
[3] Kumar S *et al.* 2019 *Phys. Scr.* **94** 075401

†E-mail: tufail2246@gmail.com

Laser-Induced,Blackbody-Radiation-Assisted Rovibrational Cooling of Linear Triatomic Molecules

B Taraphdar[1†], A Sinha[1] and N Deb[1†]

[1]School of Chemical Sciences, Indian Association for the Cultivation of Science, Kolkata 700032, India

Synopsis The preparation of state-specific molecular ions is essential for precision measurements and studies of cold ion–molecule collisions. However, ambient blackbody radiation (BBR) can drive rotational-state populations toward a Boltzmann distribution, reducing state purity within a few tens of seconds. This work investigates BBR-induced rovibrational dynamics, estimates state lifetimes, and explores cooling schemes to preserve well-defined quantum states for state-selective ion–molecule collision studies. While such dynamics and cooling schemes have been studied for diatomic, [1] symmetric-top (NH_3^+), [2] and acetylene ($C_2H_2^+$) ions, [3] linear triatomic molecular ions remain largely unexplored. This work therefore aims to extend these studies and develop strategies for maintaining rotational-state purity in such systems.

For precision measurements, ion-trap experiments, and cold ion–molecule collision studies, the preparation of molecular ions in well-defined quantum states is essential. Recent experimental studies have demonstrated that the internal quantum states of reactants can significantly influence reaction outcomes. Combining Coulomb-crystallized ions with Stark-deflected or cryogenically cooled neutral beams offers the possibility of investigating reactions involving molecules prepared in their absolute ground states. [5] Furthermore, recent advances in merged-beam experiments have opened new avenues for studying rotational-state-selective reactions. However, state-selective preparation alone is insufficient; the ions must also retain their quantum-state purity over the experimental timescale. Consequently, theoretical investigations of laser-induced cooling schemes are crucial for both the preparation and preservation of molecular ions in well-defined quantum states.

Although laser-induced control of molecular internal states has been extensively investigated for diatomic molecules, [1] symmetric-top molecules (NH_3^+), [2] as well as for acetylene ($C_2H_2^+$), [3] its application to other polyatomic systems, particularly linear triatomic molecules, remains relatively unexplored. In this work, we investigate laser-induced, blackbody-radiation-assisted (BBR-assisted) rovibrational cooling of linear triatomic molecular ions, focusing on CO_2^+ because of its relevance to astrochemistry. The CO_2^+ ion exhibits significant Renner–Teller and spin–orbit interactions and has a rotational constant of approximately $0.38\ \mathrm{cm}^{-1}$. Its ground electronic state is an inverted $^2\Pi$ state, with the rotational and electronic angular momenta exhibiting intermediate Hund's case. [4] The molecular energy levels are determined by solving the appropriate rotational Hamiltonian, accounting for the relevant interactions. The resulting energy-level structure is then used to simulate BBR-induced population dynamics by incorporating the relevant spectroscopic selection rules and transition rates into a rate-equation model. Building on this framework, we investigate laser-induced cooling schemes that exploit BBR-mediated transitions to redistribute molecular populations towards selected low-lying quantum states.

References

[1] Staanum P F *et al.* 2010 *Nat. Phys.* **6** 271–274
[2] Sinha A *et al.* 2026 *J. Chem. Phys.* **164**
[3] Deb N *et al.* 2014 *J. Chem. Phys.* **140**
[4] Herzberg G 1950 *Molecular Spectra and Molecular Structure*
[5] Willitsch S *et al.* 2008 *Phys. Rev. Lett.* **100**

†E-mail: taraphdar.brotin03@gmail.com
†E-mail: nabanita.deb@iacs.res.in

Free-Induction-Decay Atomic Magnetometer with a MEMS Cesium Vapor Cell

C Hegde[1†], T Augustin[2] and G Rajalakshmi[1]

[1]Tata Institute of Fundamental Research Hyderabad, Sy No 36/P, Serilingampally Mandal, Hyderabad 500046, India

[2]QuBeats, Institution of Eminence (IoE), University of Hyderabad, Prof. C R Rao Road, Gachibowli, Hyderabad - 500046, India

Synopsis Compact optical magnetometers are attractive for portable, unshielded applications such as geophysical surveying, biomagnetic sensing and navigation. Microfabricated vapor cells make these sensors small and scalable, while a free-induction-decay (FID) based operation gives the measurement of the field directly from the Larmor frequency. The FID magnetometers can also be operated in ambient field conditions and are self calibrating. We present our first steps towards building such a sensor and characterizing its performance.

We report the initial characterization of a free-induction-decay (FID) optical magnetometer based on a microfabricated (MEMS) Cesium vapor cell with Argon buffer gas. In this scheme, a single light beam is used both as pump and probe by separating the phases in the time domain. During pumping, atomic spin polarization is created and during the probing the spin-polarized Cesium atoms precess freely at the Larmor frequency while decaying exponentially [1]. The atomic spins are prepared by amplitude-modulated optical pumping with elliptically polarized light from a laser tuned to the Cesium D_2 line.

The light is then reduced to a weak probe level, and the resulting optical rotation is recorded with polarimetry setup. The Larmor frequency, and hence the magnetic field, is obtained by measuring the frequency of the FID signal. This system is being developed towards a compact, single beam magnetometer for Earth-field operation [2]. This experiment is ongoing, and the latest developments and results will be presented in the poster. These include temperature dependent studies for optimizing the detected optical rotation.

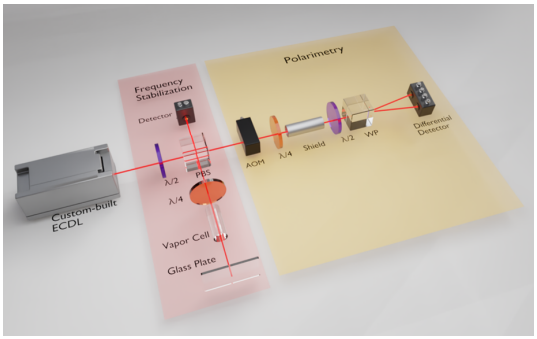

Figure 1. Optical schematic of the FID magnetometer setup. AOM: Acousto-optic modulator, WP: Wollaston Prism

References

[1] Hunter D *et al.* 2018 *Phys. Rev. Applied* **10** 014002
[2] Canciani A and Raquet J 2016 *Navigation* **63** 111

†E-mail: chandankumarh@tifrh.res.in

General Purpose, Modular and Customizable Integrated Data Acquisition and Control System (IDACS) For Charged Particle Instrumentation

Jaimin Chaudhari[1†], Shravan Kale[1], Antony Arupara[1], Malavika S[1], Nithya Sreenivasan[1], Sruthi Nair[1] and Umesh Kadhane[1†]

[1]Atomic and Molecular Physics Laboratory, Indian Institute of Space Science and Technology (IIST), Thiruvananthapuram, Kerala 695547, India

Synopsis We present the design of a general-purpose, modular data acquisition and control system that replaces the independent interfaces of individual charged-particle instruments with a single PC-controlled platform. Built around a dual-core TI microcontroller, it links isolated ADC, DAC, TDC, RF, function-generator, power-supply and digital I/O modules through separate high-speed and low-speed buses, allowing instruments to be controlled and read out from one graphical interface.

Charged-particle experiments, from electron-impact ionisation and ion spectroscopy to plasma and electric propulsion diagnostics, require many electrode potentials to be set, swept and synchronised while detector signals are recorded. In most laboratories, instruments operate independently, each relying on its own interface for control and data acquisition. This makes experiments difficult to synchronise, slow to reconfigure and hard to combine. We are therefore building a universal, modular data acquisition and control system through which various instruments can be controlled, and their signals fetched for processing, visualisation and analysis. The system is being developed to support various mass spectrometry, plasma diagnostics and charged particle optics applications at IIST.

Architecture: The system is built around a Texas Instruments (TI) dual-core 200 MHz real-time microcontroller that coordinates all modules (Fig. 1). A host PC communicates with it over USB, Ethernet or Wi-Fi, and a graphical user interface sets instrument parameters and displays the acquired data. Modules are grouped by their timing needs: time-critical modules share a high-speed SPI bus with dedicated synchronisation lines, while slow-control modules share an RS-485/232 and I^2C bus.

Signal generation and acquisition: The high-speed bus serves 20-channel, 16-bit ADC and DAC modules, a time-to-digital converter (TDC), and RF and function-generator modules required by specific experiments. A programmable clock generator (100 MHz–2.2 GHz) provides the common reference against which the TDC timestamps discriminator-generated detector pulses, enabling event synchronisation and time-resolved measurements alongside the ADC amplitude data [1].

Biasing and isolation: Low-voltage (LV) unipolar, LV bipolar and high-voltage (HV) power-supply modules on the low-speed bus bias the probes, electrodes and detectors, and are set through digital I/O modules. Because many instruments are biased with respect to floating potentials, each module is interfaced through digital isolation and powered by an isolated DC/DC converter with fuse, TVS (Transient Voltage Suppressor) and filter input protection. A hardware safety interlock acts on the power-supply modules, protecting users, instruments and the controller.

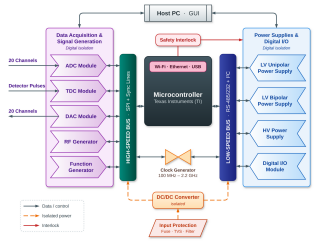

Figure 1. DAQ block diagram.

Status: The system architecture, bus layout and isolation scheme have been defined, and the ADC, DAC and TDC modules are being selected. The data acquisition chain, comprising ADC readout, data transfer to the PC and real-time processing, is under development. Once complete, the platform will be deployed, replacing their separate control and acquisition setups with a single reconfigurable system. Details of the test board and system performance results will be presented.

References

[1] Abbasi R *et al.* 2009 *Nucl. Instrum. Methods A.* **601** 294

[†]E-mail: chaudharijaimin3959@gmail.com
[†]E-mail: umeshk@iist.ac.in

Characterization of a trapped ion platform: potential, micromotion, heating, and scattering

Amit Ghosh[1†], **Sapam Ranjita Chanu**[1†]

[1]Department of Physics, IIT Kanpur, Kalyanpur, Uttar Pradesh 208016

Synopsis Here I am going to present some simulation work related to our Ion trap design. We will discuss micromotion, frequency shift, Ion scattering and vacuum design.

Among several other Quantum Computing simulation platforms, trapped-ion qubits offer several advantages, including long coherence times and very high gate fidelity. We will use a Paul trap for trapping ^{40}Ca ions. The kinetic energy of an ion has three parts: One from secular motion, one from internal micromotion (IMM), and one from excess micromotion (EMM). Here, we will present a numerical simulation study of micromotion energies for ions and their effects. If there is a static external electric field, it will displace the ion position and can give rise to excess micromotion. Excess micromotion can also be caused by a phase difference between the RF blades or by trap blade misalignment. We will also show the heating and scattering effect in a trapped ion platform.

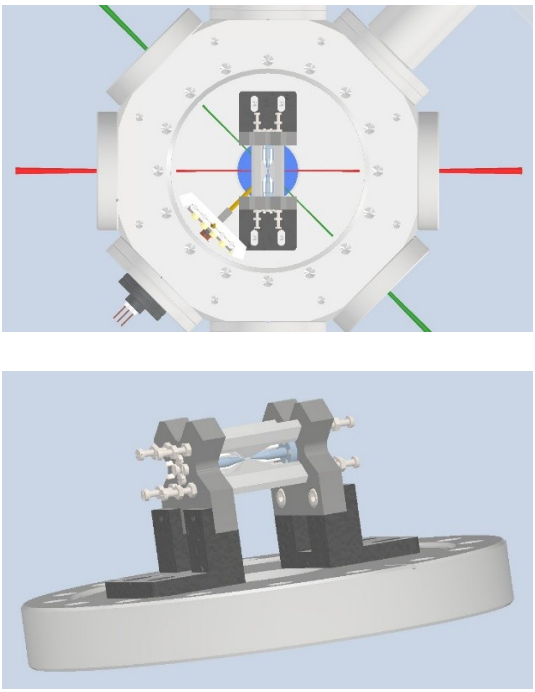

Figure 1. Ion trap geometry

References

[1] Berkeland D J, Miller J D, Bergquist J C, Itano W M and Wineland D J 1998 *J. Appl. Phys.* **83** 5025–5033

[2] Hong J, Kim M, Lee H and Lee M 2023 *Appl. Phys. B* **129** 16

†E-mail: agosh22@iitk.ac.in

†E-mail: sranjita@iitk.ac.in

Linewidth measurement of a home-built external cavity diode laser via self-heterodyne interferometry

Sucharita Sen[1] **and S Ranjita Chanu**[1,2†]

[1]Photonics Science and Engineering, Indian Institute of Technology Kanpur, Kanpur 208016, India
[2]Department of Physics, Indian Institute of Technology Kanpur, Kanpur 208016, India

Precise characterization of laser linewidth, frequency noise and stability is essential for quantum technologies such as optical atomic clocks and precision spectroscopy, where linewidth limits coherent control and gate fidelity. The delayed self-heterodyne interferometer (DSHI) [1] splits the laser output, delays one arm beyond the coherence time and recombines the two, giving a Lorentzian beat note whose width is the intrinsic linewidth. For narrow lasers this requires fiber spools tens of kilometres long, and $1/f$ frequency noise broadens the spectrum and biases the result [2, 3]. The short-delay coherent-envelope method avoids this limitation [4, 5].

For a Lorentzian laser of linewidth $\Delta\nu$ and a fiber delay τ_d, the beat-note power spectral density is $S(\nu) = S_1 S_2 + S_3$, where S_1 is a Lorentzian of width $\Delta\nu$, S_3 is a delta function at the carrier, and

$$S_2 = 1 - e^{-2\pi\tau_d\Delta\nu}\left[\cos(2\pi\tau_d\tilde{\nu}) + \Delta\nu\,\frac{\sin(2\pi\tau_d\tilde{\nu})}{\tilde{\nu}}\right], \tag{1}$$

with $\tilde{\nu} = \nu - \nu_0$. For $\tau_d\Delta\nu \gg 1$, $S_2 \to 1$ and the conventional Lorentzian is recovered. For a short fiber, S_2 oscillates and $S(\nu)$ develops a coherence envelope whose extrema lie at offsets $\Delta\nu_m = (m+2)c/2nL$, fixed only by the fiber length L and index n. The power-independent amplitude difference between the first minimum and maximum, $\Delta S = 10\log_{10}(S_H/S_L)$, is

$$\Delta S^* = 10\log_{10}\frac{\left[\Delta\nu^2 + (\frac{c}{nL})^2\right]\left[1 + e^{-2\pi\frac{nL}{c}\Delta\nu}\right]}{\left[\Delta\nu^2 + (\frac{3c}{2nL})^2\right]\left[1 - e^{-2\pi\frac{nL}{c}\Delta\nu}\right]}, \tag{2}$$

a monotonic function of $\Delta\nu$ that is solved numerically from the measured ΔS [5].

The setup is an unbalanced Mach–Zehnder DSHI. The ECDL output (780 nm, 50 mW) is split at a 50:50 beam splitter; one arm passes through a 110 MHz acousto-optic modulator, which moves the beat note away from low-frequency environmental noise, and the other through 30 m of single-mode fiber ($n \approx 1.468$). The recombined beams are detected on a 380 MHz photodiode and the beat note is recorded on an electrical spectrum analyzer (40 MHz span, 40 kHz RBW) in real-time mode. Figure 1 shows the measured spectrum with the theoretical envelope fit; from ΔS at the extrema nearest the carrier we obtain a free-running linewidth of 487 kHz.

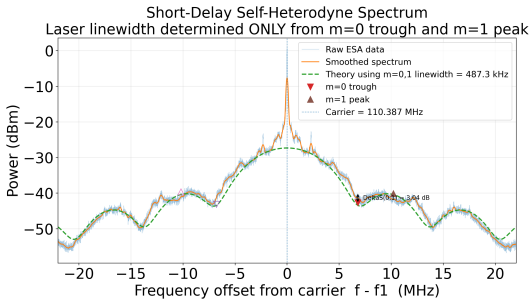

Figure 1. Measured self-heterodyne beat-note spectrum (30 m delay) with the coherence-envelope fit, giving a free-running linewidth of 487 kHz.

This short-delay method offers a simple, robust route to narrow-linewidth laser characterization for quantum technologies.

Acknowledgment: National Quantum Mission, DST, Govt. of India, and I-HUB Quantum Technology Foundation, IISER Pune.

References

[1] Okoshi T, Kikuchi K and Nakayama A 1980 *Electron. Lett.* **16** 630
[2] Richter L E, Mandelberg H I, Kruger M S and McGrath P A 1986 *IEEE J. Quantum Electron.* **22** 2070
[3] Mercer L B 1991 *J. Lightwave Technol.* **9** 485
[4] Huang S *et al.* 2016 *IEEE Photon. Technol. Lett.* **28** 759
[5] Zhao Z *et al.* 2022 *Opt. Express* **30** 30600

†E-mail: sranjita@iitk.ac.in